Atmospheric Research 281 (2023) 106509

Contents lists available at ScienceDirect

Atmospheric Research

journal homepage: www.elsevier.com/locate/atmosres

Spatio-temporal changes of spring-summer dust AOD over the Eastern Mediterranean and the Middle East: Reversal of dust trends and associated meteorological effects

Abdallah Shaheen [a,b], Renguang Wu [c], Robabeh Yousefi [a], Fang Wang [a,*], Quansheng Ge [a], Dimitris G. Kaskaoutis [d], Jun Wang [e], Pinhas Alpert [f], Iqra Munawar [g]

[a] Key Laboratory of Land Surface Pattern and Simulation, Institute of Geographic Sciences and Natural Resources Research, Chinese Academy of Sciences, Beijing, China
[b] Climate and Atmosphere Research Center, The Cyprus Institute, Nicosia, Cyprus
[c] School of Earth Sciences, Zhejiang University, Hangzhou, China
[d] Institute for Environmental Research and Sustainable Development, National Observatory of Athens, Palaia Penteli, Athens, Greece
[e] Department of Chemical and Biochemical Engineering, Iowa Technology Institute, Center for Global and Regional Environmental Research, University of Iowa, Iowa City, IA, USA
[f] Department of Geophysics, Tel Aviv University, Tel Aviv, Israel
[g] Institute for Climate and Global Change Research and School of Atmospheric Sciences, Nanjing University, Nanjing, China

A R T I C L E I N F O

Keywords:
Spring-summer aerosols
Reanalysis
Dust trends
Meteorological factors
The Eastern Mediterranean – Middle East

A B S T R A C T

High dust concentrations in the Eastern Mediterranean - Middle East (EMME) region have serious effects on air quality, human health and climate. This study used long-term aerosol datasets during the main dusty season (April–July: AMJJ) over the EMME from 2000 to 2020, based on Moderate-Resolution Imaging Spectroradiometer (MODIS)/Terra-C6.1, Modern-Era Retrospective Analysis for Research and Applications version 2 (MERRA-2), and Copernicus Atmosphere Monitoring Service Reanalysis (CAMSRA) retrievals and analyzed the spatio-temporal variations and trends of dust, as well as the influencing factors. The dust aerosol optical depth (DAOD) experienced a significant upward trend during 2000–2010, followed by a significant decrease during 2010–2017. After 2017 and till 2020, the DAOD presented rather a stable trend. Aerosol Robotic Network (AERONET) data in the EMME region display trends compatible to those of both MERRA-2 and CAMSRA DAOD. The DAOD trends were linked to changes in regional meteorological parameters in the EMME. A significant downward trend in AMJJ sea-level pressure (SLP) during the early period (2000−2010) induced hot and dry winds from desert regions towards the EMME, which reduced relative humidity (RH) and raised temperature, thus favored soil drying and dust outbreaks through enhancing evaporation. In contrast, a significant increase in winter SLP during the late period (2010–2017), accompanying an increase in North Atlantic Oscillation index, induced cold, wet winds from northwest regions, which increased RH and lowered temperature, thus reducing dust loading in EMME. Positive anomalies in winter soil moisture persisted in the following AMJJ, and consequently suppressed dust activity. DAOD variability over the dust-prone regions was linked to various meteorological parameters via a multiple linear regression (MLR) model. The results show that climatic variability strongly affects the dust trends and contribute to better understanding of meteorological – dust dynamics in the EMME region.

1. Introduction

Roughly 500 to 3000 billion tons of Aeolian dust is emitted into the atmosphere every year by the global deserts and semi-arid regions (Engelstaedter et al., 2006; Francis et al., 2020). The Middle East and North Africa (MENA) region is considered of utmost importance, as they are the major dust producers (Barkan et al., 2004; Huneeus et al., 2011). Dust has considerable impacts on the environment, climate, atmospheric chemistry and, importantly, human health (DeMott et al., 2010; Rosenfeld, 2019). In addition, dust particles can alter air temperature and

* Corresponding author.
E-mail address: wangf@igsnrr.ac.cn (F. Wang).

https://doi.org/10.1016/j.atmosres.2022.106509
Received 29 July 2022; Received in revised form 29 October 2022; Accepted 4 November 2022
Available online 11 November 2022

cloud condensation nuclei (CCN) concentrations that ultimately affect cloud properties and precipitation (Jiang et al., 2018). Several studies have investigated the dust-induced direct radiative effects through absorption and scattering of solar and thermal radiation and the indirect effect on cloud microphysics, nucleation and rainfall (Francis et al., 2021; Jin et al., 2015; Papadimas et al., 2012; Solmon et al., 2015). However, a recent study shows that dust-rainfall interactions are still of high uncertainty and not clearly understood (Alpert et al., 2021). Over the continents, dust storms can degrade soil fertility, destroy crop fields, pollute water (Thiagarajan and Aeolus Lee, 2004) and cause poor visibility (Furman, 2003), while once dust settles into the ocean, phytoplankton can bloom because of the presence of iron in the Aeolian dust (Jickells et al., 2005).

The Eastern Mediterranean and Middle East (EMME) region, which encompasses the Levantine Basin, Middle East and part of North Africa (Fig. 1), is one of the global hotspots of climate change (Almazroui et al., 2022; Alpert et al., 2006; Elhacham and Alpert, 2016; Zittis et al., 2022) and dust storm activity (Abdelkader et al., 2015; Gui et al., 2021a). Dust storms mainly occur in spring and early summer, in particular, over Iraqi, Saudi Arabian, and Libyan–Egyptian deserts (Fig. 1). By using various aerosol observational data, several studies have revealed an increasing trend in AOD over the arid EMME region during the 2000s. For instance, a positive trend in AOD was reported over the Middle East during 2001–2012 using the (SeaWiFS) Sea-viewing Wide Field-of-view Sensor (Hsu et al., 2012). Using CMIP5 models, the synoptic dust systems are projected to increase over the Middle East during the 21st century (Elhacham and Alpert, 2020). A 15% increase in dust emissions per year from 2001 to 2012 was also confirmed over the Middle East by Yu et al. (2018). Furthermore, over the Middle East a significant upward trend was detected from 2000 to 2010 by utilizing AOD from MODerate resolution Imaging Spectroradiometer (MODIS) and Modern-Era Retrospective Analysis for Research and Applications, version 2 (MERRA-2) retrievals (Lee et al., 2020; Shaheen et al., 2020; Yousefi et al., 2020a). Similarly, Klingmüller et al. (2016) also noted a positive trend in MODIS AOD over the Arabian Peninsula during 2001–2012. In contrast, a negative AOD trend was detected in the Middle East region during the last decade (Gui et al., 2022; Shaheen et al., 2020; Yousefi et al., 2020a). Previous studies noted that dust emissions over the Middle East partly recovered towards normal conditions after 2012 (Notaro et al., 2015; Yu et al., 2018). Achilleos et al. (2020) utilized satellite observations (dust-AOD) and meteorological variables in assessing the dust variability at three EMME regional background sites, Finokalia, Crete, Agia Marina, Cyprus, and Beer Seva, Israel, during 2006–2017. In general, the decadal variation in the frequency of dust events and dust-AOD at the three sites revealed a significant intra-seasonal to inter-annual variability. The only statistically significant linear trend was the decline in the number of dust events in Agia Marina, Cyprus (−6.9 dust events per year). Moreover, several other works agreed to an overall decrease in AOD and dust loading over the eastern Mediterranean from the beginning of 2000s till about 2014–2015 (Floutsi et al., 2016; Marinou et al., 2017; Pozzer et al., 2015; Yoon et al., 2014). However, the large inter-annual and intra-seasonal variability in dust-AOD and the significant spatial heterogeneity in the AOD trends require a more detailed investigation focusing on various parts (continental and marine) of the EMME region and on specific periods of highly increasing or decreasing trends in order to assess the influencing factors of these dust trends.

Meteorological dynamics and soil moisture are important factors in driving short- and long-term variability in aerosol concentrations (Barkan and Alpert, 2008; Guo et al., 2019; Wu et al., 2013). Over the Saharan and Arabian desert regions, dust loading is highly controlled by the meteorological conditions (Klingmüller et al., 2016; Krichak and Alpert, 2022). For example, a recent decline in rainfall over Gaza Strip has caused an increase in Particulate Matter (PM) concentrations (Shaheen et al., 2017). Previous studies attributed the decadal time-scale changes in dust activity over the Middle East to changes in wind speed induced by large horizontal pressure gradients related to the enhanced high-pressure system across the Mediterranean region (Mohammadpour et al., 2021; Shaheen et al., 2021a). Other studies found that inter-annual changes in dust activity across North Africa are linked to soil moisture variations, Sahel rain and vegetation cover (Foltz and McPhaden, 2008). Remotely sensed AOD measurements and surface-based dust observations revealed that soil moisture and wind speed play a key role in driving dust activity over the Northern Arabian Peninsula desert (Yu et al., 2018). Previous works (Notaro et al., 2015; Hamzeh et al., 2021) examined the drought effects on the inter-annual variations of dust loading over the Iraqi Plains, southwest Iran and Arabian Peninsula, directly impacted by the Shamal wind in spring and summer. A negative correlation was observed by Hsu et al. (2012) between SeaWiFS AOD anomalies over Iraq and Saudi Arabia and the multivariate El Niño–Southern Oscillation (ENSO) index during 1997–2012, with the index leading by one year, thus indicating that El Niño prevents dust-storm activity over the arid Middle East. Through multiple linear-regression analysis, decadal variability of dust-storm frequency was well predicted over Saudi Arabia by using surface temperature and precipitation data over the Mediterranean Sea, the Arabian Peninsula and North Africa (Yu et al., 2015).

Apart from examining the dust AOD (DAOD) trends over the EMME region that was the subject of several previous works (Klingmüller et al., 2016; Marinou et al., 2017; Pozzer et al., 2015; Yoon et al., 2014), an important scientific issue that has not been fully addressed is which factors and meteorological dynamics are responsible for the regional dust-aerosol trends during dusty period (April, May, June and July: AMJJ), and in particular, what are the reasons behind the observed reversal dust-aerosol trend mentioned in previous studies i.e., reversal of AOD trends in winter over the EMME region (Shaheen et al., 2021) and

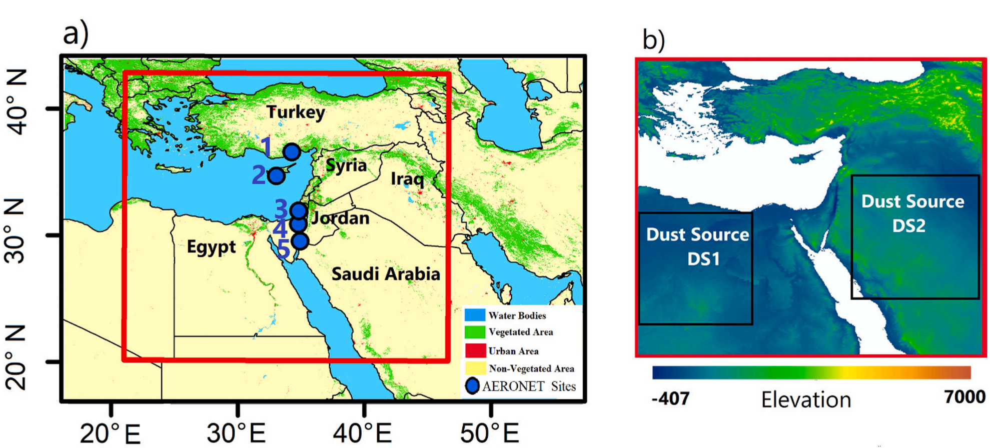

Fig. 1. (a) The study region in red box ($20–44^\circ$ N, $20–48^\circ$ E). Blue circles represent the geographical locations of the 5 AERONET stations (1) IMS-MET ERDEMLI, Turkey, (2) CUT-TEPAK, Cyprus, (3), NES-ZIONA, Israel, (4) SEDE-BOKER, Israel, (5) EILAT, Israel. (b) The 2 main dusty regions (DS 1; ($22–32^\circ$ N, $20–30^\circ$ E) and DS 2; ($24–33^\circ$ N, $38–48^\circ$ E)). The great Egypt-Libyan Desert and the Syrian-Iraqi Desert are the major dust sources in DS1 and DS2, respectively. (For interpretation of the references to colour in this figure legend, the reader is referred to the web version of this article.)

in summer over Iran (Yousefi et al., 2021a, 2021b). This work focusses on investigating the spatial and temporal variations in DAOD trends over the EMME region using MERRA-2 and Copernicus Atmosphere Monitoring Service Reanalysis (CAMSRA) products. The analysis aims to better understand the reversal trends in dust-AOD during the last two decades and the reasons that triggered the DAOD trends in the main dusty season (April to July) during the 2000s and the 2010s. The interpretation of the DAOD trends is based on an extensive multi-linear regression analysis of various meteorological parameters, including precipitation, sea-level pressure, wind, near-surface air temperature, relative humidity (RH) and soil moisture, an issue that was not explored in previous studies (i.e. Shaheen et al., 2020; Yousefi et al., 2021a, 2021b). Furthermore, this study examines the relationship between DAOD trends and meteorological factors in order to evaluate the contribution of each parameter in dust trends and to elucidate atmospheric dynamics that facilitate or prevent dust activity over the arid regions and dust accumulation over the Levantine Basin.

The rest of the article is structured as follows. Applied datasets are described in Section 2. Observed aerosols trends are analyzed in Section 3. Section 4 discusses the links of DAOD variations to sea-level pressure, rainfall, soil moisture, near-surface air temperature, wind speed, and RH. Multiple linear regression (MLR) model is employed in Section 5. Section 6 presents the conclusions.

2. Dataset

2.1. Aerosol data

NASA's Global Modeling Assimilation Office (GMAO) prepared a most recent version of MERRA-2 (Gelaro et al., 2017). It comprises Earth surface processes, ocean movement and composition of Earth's atmosphere by using distinct observation sources. The aerosol product integrates multiple AOD datasets into the Goddard-Chemistry-Aerosol-Radiation-Transport (GOCART) model. MERRA-2 data assimilates a variety of AOD datasets from different observation sources, such as the Advanced Very High-Resolution Radiometer (AVHRR), non-bias corrected AODs retrieved from Multi-angle Imaging Spectroradiometer (MISR), AERONET and MODIS (Buchard et al., 2017). Various meteorological products and AODs for different aerosol types are also provided by MERRA-2, i.e., sea salt, organic and black carbon, dust and sulfate (Kalita et al., 2020). Several previous studies used MERRA-2 aerosol data to investigate long-term AOD trends (Provençal et al., 2017; Shaheen, 2020) and DAOD variability (Liu et al., 2021) due to satisfactory agreement between MERRA-2, MODIS and AERONET AOD datasets (Shi et al., 2019; Shaheen et al., 2020; Ukhov et al., 2020). To examine dust aerosol trends over the EMME region, monthly AOD_{550}, DAOD and dust concentration data during 2000–2020 were used (Table S1).

Compared to earlier data products, recent ECMWF reanalysis of atmospheric composition (CAMSRA) *shows lower AOD biases and covers a longer time period (*Inness et al., 2019*). The ECMWF Integrated Forecast System (IFS) was expanded to incorporate a completely integrated atmospheric composition modeling (comprising aerosol modules and independent chemistry) and data integration of aerosols, AOD and chemically responsive gases (*Flemming et al., 2015*)*. Aqua and Terra satellites carrying MODIS (Collection 6.1) were integrated into the *IFS atmospheric model (*Inness et al., 2019*)*, and AOD retrievals from 2003 to March 2012 were also used from the Advanced Along-Track Scanning Radiometer (AATSR) onboard Envisat. The main purpose of developing CAMSRA was to reduce the potential changes produced by integrated satellite products and emissions thereby securing the temporal consistency of the dataset (Liu et al., 2021). In order to analyze the dust aerosol trend over EMME region, both DAOD and AOD_{550} data from CAMSRA were assessed in this work (Table S1).

MODIS onboard TERRA satellite, with 2330 km swath width and consideration of 36 spectral bands, observes the Earth in varying wavelength ranges (King et al., 2003). Here, the level-3 monthly Combined Dark Target - Deep Blue AOD (DTDB) MOD-08 at 550 nm product is used. This data is available at $1^{\circ} \times 1^{\circ}$ spatial resolution, while the mean absolute error in AOD values is about 0.075 (Remer et al., 2005). About 75% of MODIS daily AOD values fall within the range of expected errors (Gui et al., 2021b). Table S1 provides comprehensive details regarding MODIS aerosol datasets employed in this study.

Sun photometers CIMEL-318 are used in Aerosol Robotic Network (AERONET) to obtain AOD observations at several stations in the EMME region (Tutsak and Koçak, 2020). Sun photometers observe solar irradiances every 15 min using different wavelengths (Holben et al., 1998), and probable error of ± 0.01–0.02. AERONET provides Ångström Exponent ($AE_{440–870}$), Fine Mode Fraction (FMF_{500}), and AOD_{550} values. In this study, the analysis focuses on level 2 and version 3 of the monthly mean FMF_{500}, $AE_{440–870,}$ and AOD_{500} from 5 AERONET sites in the EMME region (SEDE-BOKER, NES-ZIONA, IMS-MET ERDEMLI, CUT-TEPAK and EILAT). Detailed descriptions and site locations are specified in Table S1 and Fig. 1, respectively.

2.2. Meteorological data

Meteorological data are retrieved from the latest ECMWF ERA5 reanalysis, which includes numerous advancements in the reanalysis products (Hersbach et al., 2020; Tarek et al., 2020; C. Wang et al., 2019). ERA5 provides data at 1 h interval and ~ 30 km resolution for a wide range of earth and atmospheric variables. In previous works, meteorological parameters from ERA5 have been assessed and cross-checked using various observation data with good agreement (Baudouin et al., 2020; Gleixner et al., 2020; Mohammadpour et al., 2021; Tarek et al., 2020). In addition, ground-based data from developed countries in EMME (i.e., Israel, Greece, and Turkey) were assimilated by ERA5 (https://www.ecmwf.int/). Monthly meteorological data from ERA5 global reanalysis during 2000–2018 are employed in the present study. In addition, the North Atlantic Oscillation Index (NAOI) data (www.cpc.ncep.noaa.gov/; Hurrel, 1995) were also used to explore possible relationship with DAOD variability and trends over EMME. Comprehensive information about analyzed variables is provided in Table S1.

3. Aerosol trends

Data from MERRA-2, ERA5 and CAMSRA was bilinearly interpolated to MODIS grid ($1^{o} \times 1^{o}$) for comparing aerosol trends and carrying out a consistent regression analysis. A technique widely implemented for time-series analysis is the least-square linear regression (Gui et al., 2019; Shaheen et al., 2020, 2021b; Yousefi et al., 2020b). This method is used in the present study to obtain the long-term trends of MERRA-2, CAMSRA and MODIS AODs (monthly time series data) for the dusty months AMJJ over the EMME region (red box in Fig. 1). Prior to the regression, long-term averages were extracted from the original data. In this work, two-tailed Student's *t*-test is utilized to examine the strength of estimated trends, and the criterion for statistical significance was set at ($p < 0.05$). As shown in Fig. 2a, the linear trends of the mean AMJJ AOD anomalies were extracted and averaged over EMME using MODIS, CAMSRA, MERRA-2 data.

An overall positive trend in AOD is seen over the region ($p < 0.05$) from 2000 to 2010, with rates of 0.007 per year (MERRA-2 AOD) to 0.005 per year (MODIS AOD) (Fig. 2a). Similarly, a positive trend is found during 2003–2010 from CAMSRA data with a rate of 0.007 per year (Fig. 2a). Conversely, a significant reversal in AOD trends is observed for the period 2010–2017, during which CAMSRA, MERRA-2 and MODIS AODs display comparable negative trends of $-0.009\ yr^{-1}$, $-0.012\ yr^{-1}$ and $-\ 0.011\ yr^{-1}$, respectively (Fig. 2a). However, a slight increasing tendency is observed after 2017, and the annual-mean AODs from MERRA-2 and CAMSRA observations were higher in 2018. On the other hand, this period is too short for the extraction of robust results about the significance of the AOD trends, while MERRA-2, CAMSRA and MODIS data showed rather stable AOD tendency during 2018–2020.

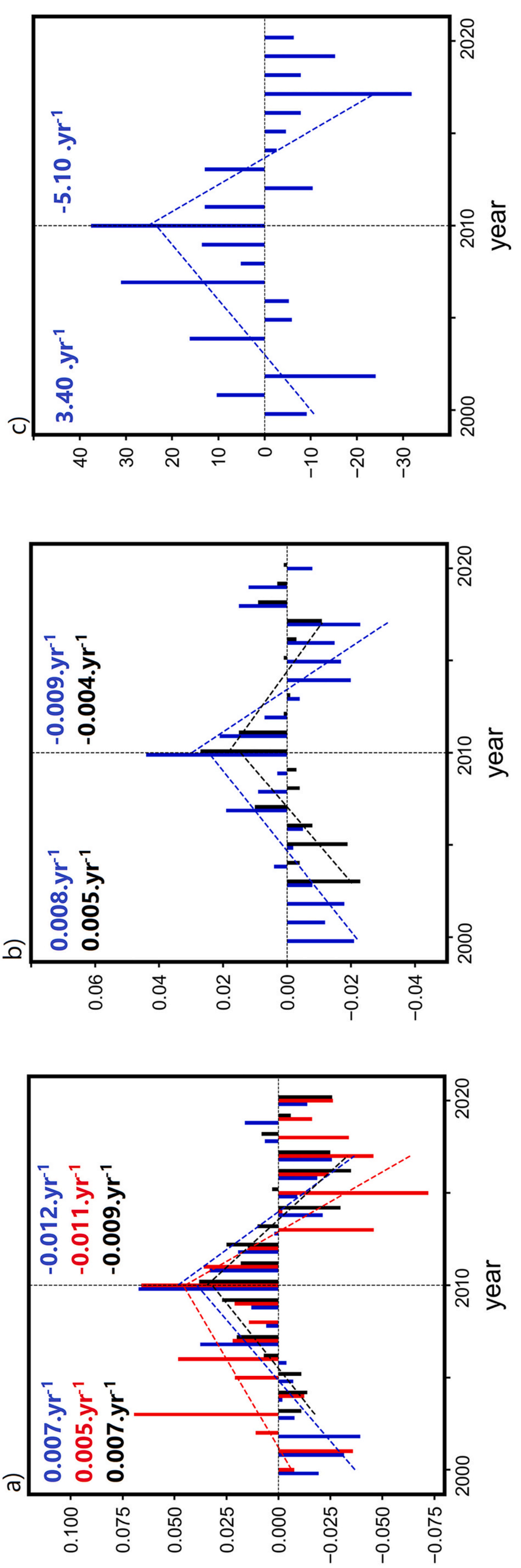

Fig. 2. Time series of the spatial averaged over the EMME region for (a) AMJJ AOD mean anomalies from MERRA-2 (blue) during 2000–2020, MODIS (red) during 2000–2020, and CAMSRA (black) during 2003–2020 data, (b) AMJJ DAOD from MERRA-2 (blue) during 2000–2020 and CAMSRA (black) during 2003–2020, (c) AMJJ dust concentration from MERRA-2 during 2000–2020. Dash lines represent the trends ($p < 0.05$) during the first till 2010 and second till 2017 periods. (For interpretation of the references to colour in this figure legend, the reader is referred to the web version of this article.)

Therefore, for the whole analysis, we divided the study period into two sub-periods, i.e., 2000–2010 as the early period and 2010–2017 as the late period.

The AMJJ DAOD variability and trends from MERRA-2 and CAMSRA data (Fig. 2b) exhibit very similar patterns with AOD, with an increasing trend ($p < 0.05$) during 2000–2010 and a decrease in 2010–2017. The rates in DAOD changes are similar to those for AODs, ranging from 0.004 yr^{-1} to 0.008 yr^{-1}. Furthermore, the trends in the spatial-averaged surface dust concentration data from MERRA-2 datasets (Fig. 2c) showed a significant increase from 2000 to 2010 and a decrease afterwards, indicating that annual and multi-decadal strong variabilities in dust loading at the lower atmosphere is responsible for the variability and trends in columnar dust or total AODs over the EMME region.

The spatial distributions of AMJJ AOD trends for the whole period, early period, and late period from MODIS and MERRA-2 datasets are shown in Fig. 3. For the whole period, MODIS and MERRA-2 AODs exhibited an insignificant trend over the study domain (Fig. 3a, d), as also observed from the CAMSRA AOD for the period 2003–2017 (Fig. 3g). These insignificant trends are the result of the contrasting AOD trends during the first and second periods, while significant decline in AOD trends are shown over the southeastern Europe, in consistency with previous studies (Floutsi et al., 2016).

During 2000–2010, positive trends ($p < 0.05$) of MODIS and MERRA-2 AOD spread over extensive desert areas in the Middle East (Syrian-Iraqi, An Nafud, Al Dhana Deserts, along with the east Libyan Desert) (Fig. 3b, e), and same trend pattern is noted in the CAMSRA AOD during 2003–2010 (Fig. 3h). These positive trends are consistent with the results by Klingmüller et al. (2016). Reversely, negative AOD trends are shown during the 2000s over Greece and the East Mediterranean, which have been well documented in a series of previous papers that attributed this declining trend to cleaning practices in Europe and absence of severe dust activity (Achilleos et al., 2020; Floutsi et al., 2016; Georgoulias et al., 2016; Papadimas et al., 2012). Similarly, AOD times series during 1982–2007 showed a clear decreasing trend of −0.0023 per year over the Mediterranean Basin, which could be explained by decreasing levels of sulfate due to fuel desulfurization strategies in Europe (Nabat et al., 2014). Georgoulias et al. (2016) also found statistically significant negative trends in AOD over the Mediterranean, Egypt and Algeria and positive trends over the Middle East using MODIS (both Terra and Aqua) observations. They reported an overall AOD trend of −0.0020 yr^{-1} based on Aqua (2002–2015) and − 0.0008 yr^{-1} based on Terra (2000–2015) in the Mediterranean Sea, both statistically significant at the 95% confidence level. Other spatially-averaged decreasing AOD trends over the whole Mediterranean Basin have been noted with an average decrease in AOD of −0.0067 $year^{-1}$ during 2000–2006 using Terra-MODIS observations (Papadimas et al., 2008), of −0.003 per year (−19% during 2002–2014), based on Aqua-MODIS AODs (Floutsi et al., 2016). Therefore, the declining AOD trends over the Mediterranean were more likely attributed to the decreasing emissions of anthropogenic aerosols due to several national strategies and actions in European countries for reducing aerosol emissions. During the second period (2010–2017), significant downward trends were found in MODIS, MERRA-2 and CAMSRA AODs over large parts of the study domain, in particular over Iraq and desert regions in Egypt and Saudi Arabia, with statistically significant negative trends (Fig. 3c, f, i).

The small differences in the spatial distribution and magnitude of trends between the datasets are probably attributed to the algorithms used by each remote sensing and reanalysis technique, and the presence of haze and clouds, which may cause some uncertainties in aerosol retrieval from satellite observations. Additionally, some gaps may occur in the MODIS AOD dataset because of bright surfaces or cloud contamination (Che et al., 2019; Gui et al., 2021b).

In the EMME region, there are several AERONET stations, five of which provide data records for a long period (2000–2017). A trend analysis was performed for FMF_{500}, $AE_{440-870}$, and AOD_{500} in AMJJ at these stations, and the AOD trends during 2000–2017 are shown in

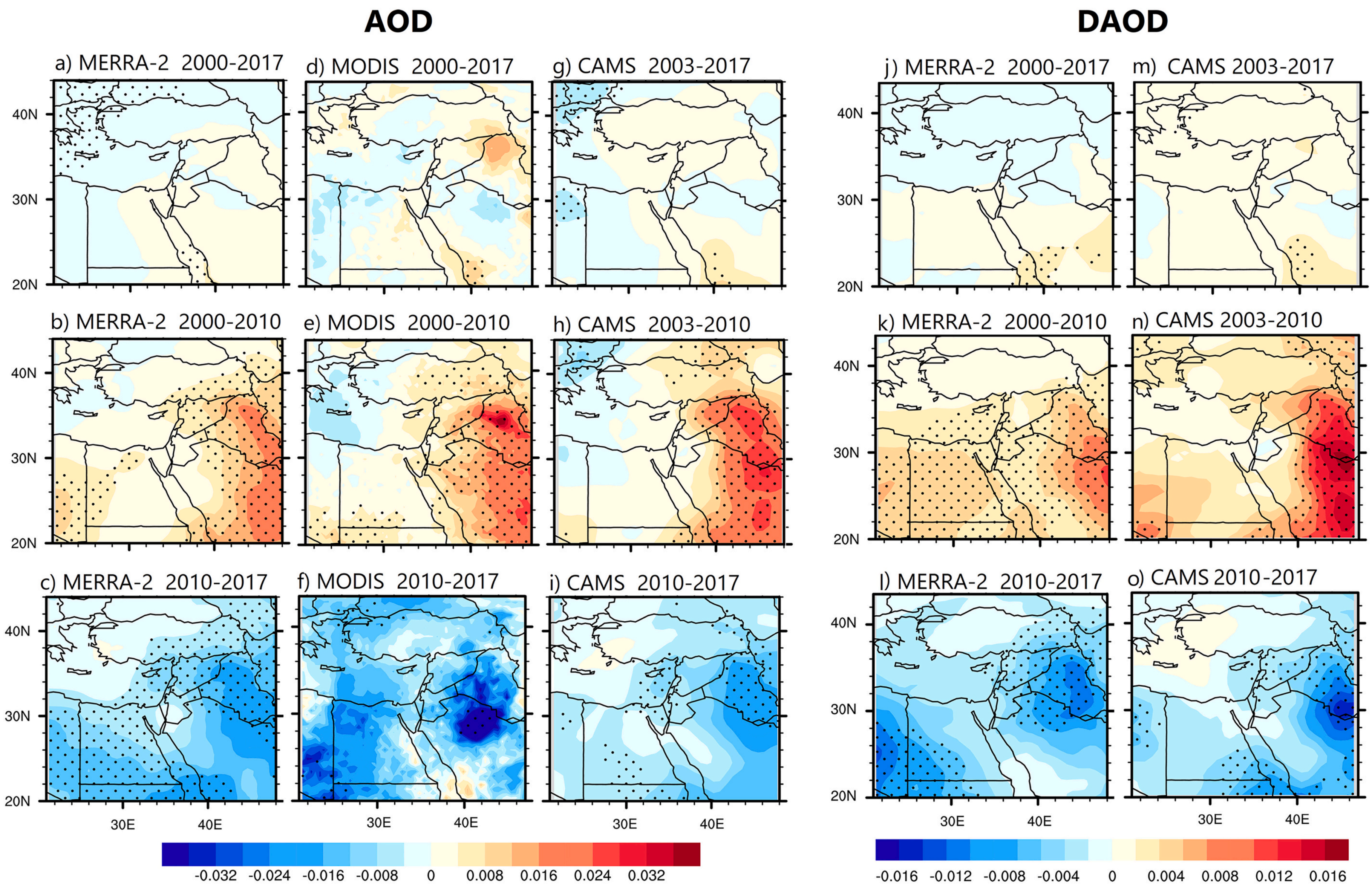

Fig. 3. Spatial distributions of AMJJ AOD trends from MERRA-2 (a, b, and c), Terra-MODIS (d, e, and f), and CAMSRA (g, h, and i) during the selected periods. Similarly, AMJJ DAOD trends from MERRA-2 (j, k, and l) and CAMSRA (m, n, and o). Black dots denote statistically significant trends at 95% confidence level ($p < 0.05$).

Fig. S1. A comparison between Figs. 2 and S1 indicates that AERONET AOD trends showed a fair agreement with AOD trends from MODIS, MERRA-2 and CAMSRA. In coarse size mode, the AE measurements showed notable changes in aerosol loadings, emphasizing the key role of dust in the AOD variability. As shown in Fig. S1, similar results were observed from the analysis of AERONET FMF_{500}, with a negative trend and a positive trend in the early and late periods, respectively, indicating a decrease and increase in coarse-dust aerosols over the stations and highlighting dust as the most influencing component for the aerosol trends. Previous studies based on AERONET observations in the Mediterranean examined the long-term trends in AOD, mostly confirming the decreasing trends observed via satellite remote sensing during the 2000s (Yoon et al., 2014).

Over the Eastern Mediterranean, PM loading is mostly associated with dust particles (Achilleos et al., 2020; Pey et al., 2013), while over the Southern parts of the EMME region, MODIS AE and FMF data justify the dominance of dust (Floutsi et al., 2016). The MODIS-derived FMF experienced a decrease (−0.06 per decade) during 2002–2014 over the greater part of the Mediterranean Sea, reflecting the decreasing contribution of the fine anthropogenic emissions (Floutsi et al., 2016). Using a least-square method, correlation analysis was performed between MERRA-2 dust concentration and the MERRA-2, MODIS and CAMSRA AODs. The spatial distribution of the correlation coefficient (R) values over EMME is shown in Fig. S2. Large positive R values ($p < 0.1$) were seen over most parts of the studied domain, indicating that dust emissions substantially contributed to the total AOD.

The spatial distributions of the DAOD trends from CAMSRA and MERRA-2 during 2000–2017 and the two sub-periods are shown in the right part of Fig. 3. During the early period (till 2010), most of the significant increasing trends occurred over the desert areas in the EMME region and, in particular, over Iraq and northernmost Saudi Arabia. Previous studies detected significant increasing DAOD trends over the Middle Eastern desert areas from mid to end of the 2000s, then partly recovered towards normal conditions (Hamzeh et al., 2021; Notaro et al., 2015). Conversely, the DAOD values presented strong decreasing trends during 2010–2017, especially over Iraq, after the recovery of the extreme drought conditions (2007–2010; Notaro et al., 2015), while significant decrease in dust activity and DAOD is also observed over east Libya and Egypt, which drove the declining DAOD trend over the East Mediterranean (Fig. 3l, q). The similarity in the trends between AOD and DAOD (Fig. 3) indicates that dust contributes the most to the total AOD over the Middle East. This was also supported by the trend analysis in the fine dust concentrations obtained from MERRA-2 (Fig. S3). Both coarse and fine dust concentrations exhibited a positive trend during 2000–2010, particularly over the Syrian-Iraqi and Egyptian Deserts, followed by a negative trend during 2010–2017, while in both cases the highest trends were observed in coarse dust particles (Fig. S3).

Synoptically, the analysis indicates that the dust-aerosol loading in the EMME region showed reversed trends during 2000–2017, largely dominated by the coarse dust component over major hotspot regions. Our findings are in agreement with results from previous studies (Hsu et al., 2012; Pozzer et al., 2015; Yoon et al., 2014), indicating declining AOD and dust-AOD trends over the eastern Mediterranean basin during the 2000s based on several satellite sensors (MODIS, MISR, SeaWiFS). Furthermore, Marinou et al. (2017) examined the long-term dust variability based on CALIPSO observations and reported a decrease of −4% yr^{-1} in dust-AOD over the eastern Mediterranean during 2007–2015. In Cyprus, an annual increase in transported dust was reported from 2000 to 2010 ($p = 0.04$) and in dust-AOD from 2009 until 2013, but no statistical trend in dust activity was found during 2000–2017 (Achilleos et al., 2020). Moreover, an increasing trend in dust frequency was previously reported over Israel from 1958 to 2006 (Ganor et al., 2010) and during 2001–2015 (Krasnov et al., 2016). However, previous studies did not follow a uniform methodology for the definition of dust events at individual sites and for the long-term analysis of their frequency and intensity evolution, while the trends were highly influenced by meteorological patterns and drought conditions that escalated dust activity over the area. Therefore, in the following, we investigate the trends in meteorological variables that are likely linked with dust emission rates in the desert areas.

4. Response of dust-AOD trends to meteorology

Inter-annual to intra-seasonal variations in dust activity over Sahara and the Middle East are driven by various factors, namely local and regional atmospheric circulation patterns, surface winds, rainfall, convection and advection, as well as land use changes (Bryant, 2013; Schepanski et al., 2009). In this section, regional patterns of several meteorological variables are examined and compared with the DAOD trends during the dusty season for both periods using linear regression and correlation analyses. The meteorological variables include sea-level pressure, total precipitation, relative humidity, surface air temperature, near-surface wind speed, and soil water content.

4.1. Precipitation

Precipitation impacts dust loading through various mechanisms. Rain scavenging contributes to a direct aerosol removal from the atmosphere (rainy washout), while precipitation also regulates soil moisture and vegetation abundance, thus indirectly affecting dust emissions (Parajuli et al., 2019). Hence, total precipitation trends in the dusty period (AMJJ) and prior to the dusty season (DJFM) can provide essential information relevant to the variations in DAOD. To examine the precipitation effect on DAOD trends over the EMME region, ERA5 precipitation data is used. Fig. 4 shows the trends in total precipitation (spatial distribution) in AMJJ and DJFM during both periods, obtained by an analysis similar to that for the DAOD.

Significant positive precipitation trends were observed over the dusty areas of the Arabian Peninsula and Iraq during the dusty season from 2000 to 2010 albeit the small increasing rates due to very low rainfall amount over the deserts (Fig. 4a). A significant positive precipitation trend during 2010–2017 is found over parts of the southern areas in the study domain, while the eastern part exhibits a negative trend. Therefore, total AMJJ precipitation trends are not uniform across the EMME region, with higher negative trends over Turkey and the East Mediterranean due to larger rainfall amounts (Fig. 4b). The results suggest that precipitation, albeit important, is not the main regulating factor for the trend in DAOD over the EMME region. Furthermore, as the precipitation rate changed only marginally by −0.56 mm $month^{-1}$ per decade (−1.3% during 2002–2014) over the Mediterranean (Floutsi et al., 2016), wet deposition cannot be considered as a major process affecting the decreasing trend in AOD. However, over the Saudi Arabian deserts, a significant precipitation increase is observed during 2010–2017 in DJFM (Fig. 4d), which may have a negative feedback on dust emissions during the following dusty period, thus contributing to the declining dust trend during the second period.

To further inspect the role of total precipitation in affecting DAOD trends, correlation analysis was performed between DAOD and total precipitation for both periods AMJJ and DJFM (Fig. 5, b). The correlation of DAOD with AMJJ precipitation was mostly insignificant (Fig. 5a), suggesting that DAOD variations are not affected by the AMJJ precipitation This result supports our previous statement that precipitation variations may have an effect on DAOD trends, but the role of precipitation is not a major one in determining the DAOD trends. This is consistent with prior studies focusing, for example, on some areas of Iraq and Saudi Arabia (Klingmüller et al., 2016), where precipitation had an influence in AOD variability, but the effects from other parameters were also significant.

Conversely, a negative correlation was found between DJFM precipitation and subsequent AMJJ DAOD over a large part of the Saudi Arabian deserts (Fig. 5b). This suggests that winter precipitation plays a role in regulating AMJJ dust loadings via the indirect effect of increasing

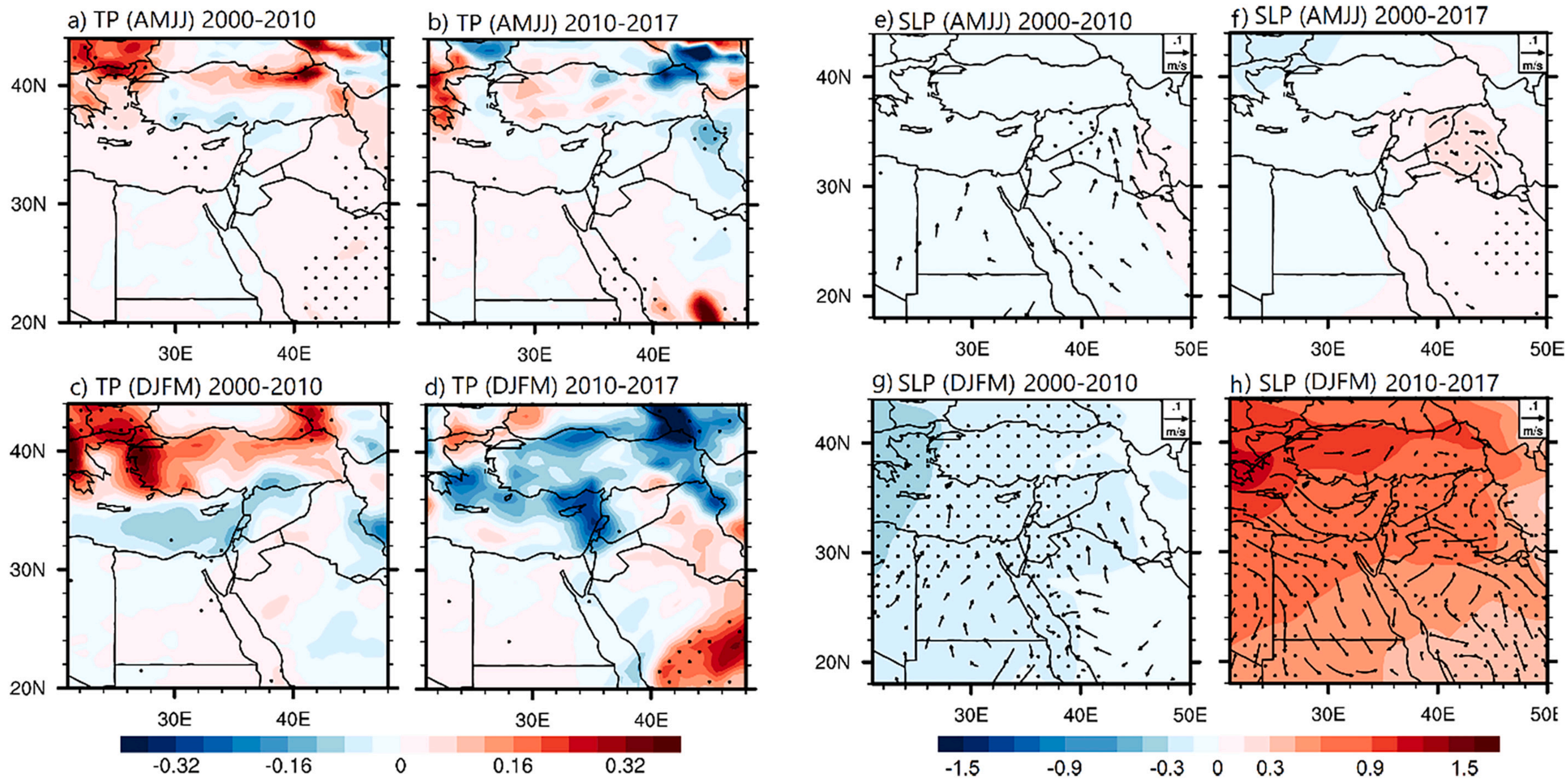

Fig. 4. Spatial distributions of ERA5 total precipitation linear trends (mm yr^{-1}) for monthly anomalies in AMJJ during (a) 2000–2010 and (b) 2010–2017, and in DJFM during (c) 2000–2010 and (d) 2010–2017. Same trends for sea-level pressure (shading; hPa yr^{-1}) and wind speed at 10 m (vector with scale at top-right corner; m s^{-1}) in AMJJ during (e) 2000–2010 and (f) 2010–2017, and in DJFM during (g) 2000–2010 and (h) 2000–2017. Black dots denote the significance of the trend ($p < 0.05$). Only significant wind changes ($p < 0.05$) are shown.

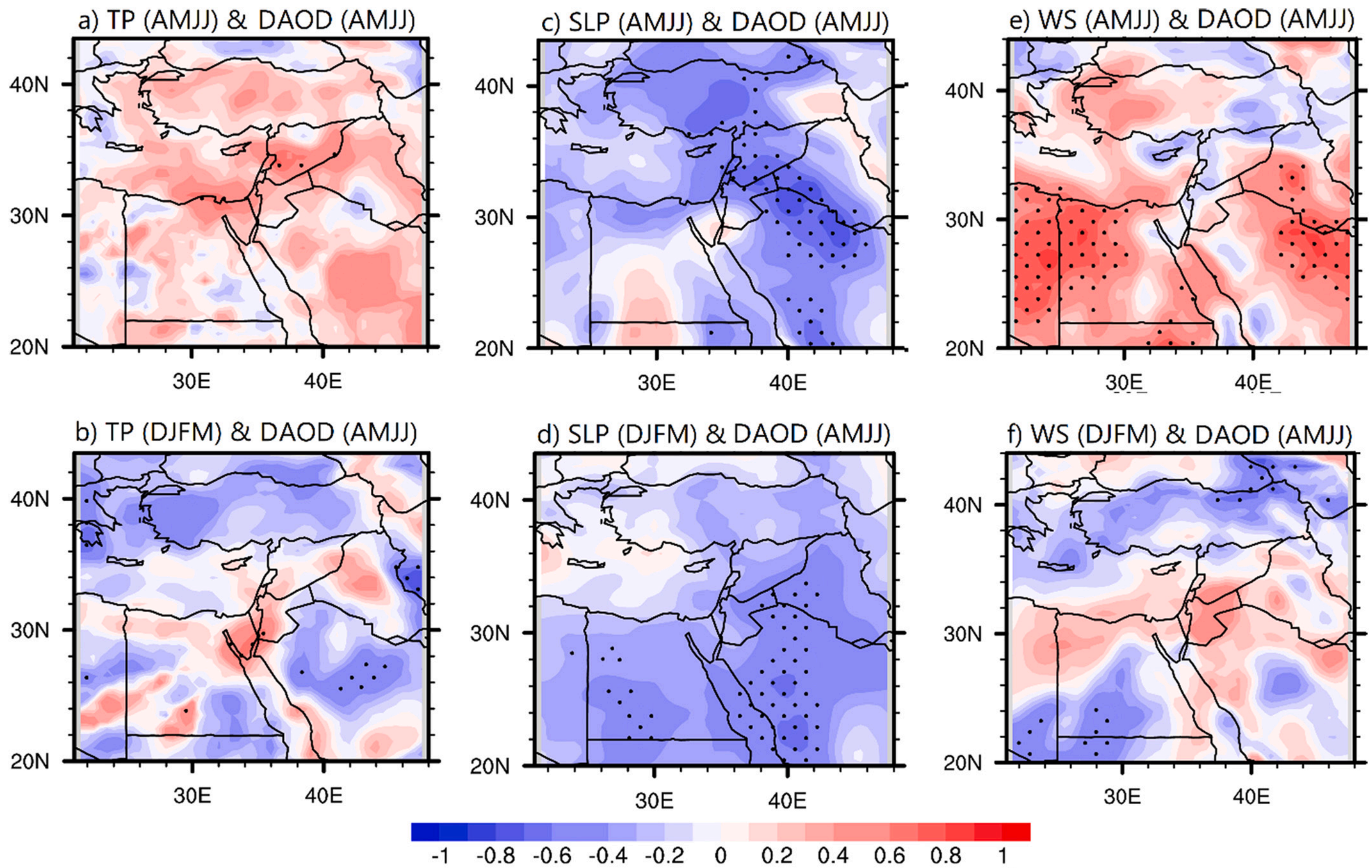

Fig. 5. Spatial distributions of the temporal correlations using MERRA-2 DAOD during 2000–2017 between (a) precipitation and DAOD during AMJJ, (b) DJFM total precipitation and subsequent AMJJ DAOD, (c) AMJJ SLP and AMJJ DAOD, (d) DJFM SLP and subsequent AMJJ DAOD, (e) AMJJ wind speed and AMJJ DAOD, and (f) DJFM wind speed and DAOD. Black dots indicate significant correlations at 90% confidence level ($p < 0.1$).

soil water content in spring and summer (see Section 4.4). Our findings are consistent with those of Yu et al. (2015) who found that precipitation in February affected the dust frequency over the Arabian Peninsula in the following spring season. Nonetheless, over the EMME region, DAOD trends cannot be attributed to precipitation trends alone.

4.2. Sea-level pressure and wind

Sea-level pressure (SLP) plays a significant role in Aeolian dust emissions via affecting near-surface and vertical wind, as well as cloud cover (Francis et al., 2020). Shao et al. (1993) discussed the processes via which surface wind impacts dust emissions through the saltation bombardment. In order to examine the role of this process, we analyzed the trends in AMJJ SLP and 10-m wind speed obtained from ERA5 in the early and late periods (Fig. 4e-h). A negative AMJJ SLP trend was identified during 2000–2010, which is statistically significant over parts of the Syrian-Iraqi Desert (Fig. 4e). A similar decreasing trend in SPL during the winter (DJFM) period 2000–2010 is also observed, which is statistically significant over the Levantine Basin, suggesting enhanced cyclonic activity over the EMME (Fig. 4g). During 2000–2010 (period of DAOD increase), this decrease in SLP was accompanied by highly variable winds (southeasterly and southwesterly) over the EMME region, which transferred dry and dusty air masses from the deserts at lower latitudes (south Arabian Peninsula and Sahara). Conversely, SLP presents a positive significant trend during 2010–2017 over a wide area covering the deserts of Saudi Arabia and Iraq (Fig. 4h), which favored anticyclonic conditions over the region that, in turn, may prevent dust advection.

The spatial distributions of DAOD and SLP displayed a significant negative correlation in AMJJ over the Saudi Arabian, Syrian and Iraqi deserts (Fig. 5c). This suggests that SLP is one of the key important meteorological factors that regulates DAOD variability over the EMME region, while a similar spatial pattern was observed between DAOD and SLP in DJFM (Fig. 5d). Therefore, increased cyclonic activity (lower SLP values) is associated with higher DAOD, indicating increased dust activity over the Middle East (Francis et al., 2019). On the contrary, over the Egyptian, Iraqi and Saudi Arabian deserts, wind speeds are positively correlated with DAOD (Fig. 5e), as expected. Several previous studies showed that the wind speed strongly affects DAOD variability in spring and summer over the desert areas (Hamidianpour et al., 2021; Parajuli et al., 2019). Especially in the EMME region, dust-storm events are strongly associated with intense wind speed phenomena, i.e., Shamal, Khamsin and Simoon winds (Abdelkader et al., 2015; Solomos et al., 2018; Yu et al., 2016). These findings corroborate previous works that highlighted the important role of SLP and wind speed and direction in regulating the dust loading over EMME (Abdelkader et al., 2015; Che et al., 2019; Hamidi et al., 2013; Kaskaoutis et al., 2016; Rashki et al., 2012; Shaheen et al., 2021a; Yousefi et al., 2021a; Yu et al., 2016). Hence, intra-seasonal to inter-annual variations in wind regimes over the EMME desert regions trigger the long-term changes and trends in dust emissions and accumulation.

Variations in winter SLP and wind speed may also be associated with variations in AMJJ DAOD via indirect influencing factors (e.g., through changes in soil moisture, caused by increased precipitation). Therefore, regression and trend analysis were performed, also using DJFM meteorological variables. The results revealed significant negative winter SLP trends over wide parts of the study domain, in correspondence with strong southeasterly and southwesterly winds during 2000–2010 (Fig. 4g). After 2010, SLP displayed a strong increasing trend along with escalation of northwesterly winds over Egypt and southerlies over the

Mesopotamian plains (Fig. 4g), revealing a tendency opposite to that observed during the 2000s, which may affect other meteorological parameters like precipitation and, in turn, dust activity in spring season. During DJFM, high pressure systems transfer cold and wet air masses from higher latitudes (Labban et al., 2021), which pass over water bodies (Caspian Sea, Black Sea eastern Mediterranean) and vegetated regions, thus increasing soil water content and may affect dust production in the following AMJJ. In that matter, a significant negative correlation was found between the DJFM SLP and subsequent AMJJ DAOD over most part of the study domain (Fig. 5d), while the correlation was insignificant for winter wind speed, with large spatial heterogeneity (Fig. 5f). More detailed analysis about the impact of winter meteorology on AMJJ soil moisture is included in section 4.4.

Overall, SLP variations, large-scale teleconnection patterns and changes in the wind regime are major modulating factors for the climate in the EMME region, as well as for short- and long-term changes in dust activity (Alonso-Perez et al., 2011; Gandham et al., 2020; Salvador et al., 2014; Zhao et al., 2013). In this respect, Nabat et al. (2014) reported that 4 typical regional weather types, namely blocking, Atlantic ridge, NAO$^+$ and NAO$^-$ (positive and negative phases of the NAO index, respectively), can be associated with variability in dust activity in the Mediterranean region. At seasonal and inter-annual time scales, the dust activity is majorly affected by changes in the synoptic meteorology and large-scale circulation patterns like NAO over the Mediterranean (Dayan et al., 2008; Ganor et al., 2010; Pey et al., 2013; Sciare et al., 2003) and the Caspian Sea–Hindu Kush Index (CasHKI) over east Iran (Kaskaoutis et al., 2016). To investigate the effect of different synoptic patterns on DAOD variability and trends in the EMME region, an analysis was performed for SLP and 500 hPa geopotential height trends during the early and late periods over a wider spatial domain, covering, apart from the EMME region, the Western Europe, Central and North Asia, North Africa and the North Atlantic Ocean (Figs. S4 and S5). NAO is a teleconnection pattern determined from fluctuations in the difference of SLP among Icelandic Low and Azores High (Hurrel, 1995; Dayan et al., 2008). NAO variability modulates the cyclonic activity and determines the movement and strength of westerly winds over western Europe and the whole Mediterranean Basin (Papadimas et al., 2008). Positive NAO causes an increase in westerlies and as a result, summers are cool and winters are moist and mild in Central Europe and its Atlantic facade. This NAO phase also facilitates decreased storm activity over North and central Africa. Nabat et al. (2020) revealed a rather negative association between NAO, total AOD and dust AOD in winter, especially over eastern Mediterranean, while during summer, NAO was positively related with AOD and marginally with dust over the Mediterranean. On the contrary, the negative NAO phase results in warmer conditions over Sahara and colder ones over Europe, increased cyclonic activity, intensified westerlies and dust accumulation increase over the eastern Mediterranean basin (Kaskaoutis et al., 2019).

The SLP over the NAO-related area revealed a slight increasing trend over Iceland and a respective declining tendency over Morocco during the first period (2000–2010), and a reversal afterwards (2010–2017) (Fig. S4), leading to decreasing and increasing trends in NAO Index, respectively, while similar patterns – associated with larger variations – were observed during winter (Fig. S4). Similar trends were observed in the upper-level (500 hPa) atmospheric patterns, with a slight decreasing trend in geopotential heights over the Mediterranean in AMJJ and DJFM during 2000–2010 and an increase in 2010–2017 (Fig. S5). Such reversal trends in lower- and upper-atmospheric patterns may justify the changes in dust activity in the EMME region between 2000 and 2010 and 2010–2017. Hence, we also considered winter (DJFM) NAOI data in our analysis. The winter NAOI during 2000–2010 (2010–2017) exhibited negative (positive) linear trends (Fig. S6) and a significant negative correlation with the DAOD (−0.52) and dust concentration (−0.65). These results are consistent with those of previous studies revealing that NAO-related strong pressure gradients over the subtropical and North Atlantic during winter and early spring impact Sahara dust activity (Dayan et al., 2008; Ginoux et al., 2004), while in March 2018, a negative NAO phase was linked with abnormal dust activity over Greece and the eastern Mediterranean (Kaskaoutis et al., 2019).

4.3. Surface air temperature and humidity

Surface RH and air temperature are two important factors affecting aerosol and, in particular, dust loadings through several indirect land processes (Schepanski et al., 2016; Gholami et al., 2021; Yousefi et al., 2021b). Dust emission is favored by a suitable environment of high temperature and dry desert air conditions. Trends in surface RH and air temperature obtained from ERA5 over the EMME region in the two periods are shown in Fig. 6. From 2000 to 2010, a significant air temperature rise is observed above the dustiest areas of the region (Fig. 6a). Significant negative RH trend is noted over Egypt during the early period, yet such trends over the Saudi Arabian and Iraqi deserts are insignificant (Fig. 6e). During the early period, air temperature trends coincide with the DAOD increase, while the negative RH trends are consistent with DAOD trends only over the Libyan-Egyptian deserts.

Over most parts of the study region, trends in air temperature and RH are insignificant during the late period. During this period, the air temperature and RH trends in AMJJ are not so consistent with the reversal of the DAOD trend, since a large decrease in dust activity would be expected to follow lower temperatures and larger RH values over the dust hotspot regions. Therefore, we also analyzed the contribution of the air temperature and RH trends during DJFM to the subsequent AMJJ DAOD trend. Over a large part of the region, we found significant positive and negative winter air temperature trends in the early and late periods, respectively (Fig. 6c, d), while RH trends were negative in 2001–2010 (increase in spring dust) and positive in 2010–2017 (decrease in spring dust) (Fig. 6g, h). Therefore, the winter humidity trends appear to be consistent with the trends in AMJJ DAOD.

Quantitative analysis shows that the AMJJ air temperature trend is correlated with the trend in DAOD only over small parts of the study region, surrounding the Red Sea (Fig. 7a), while the DJFM air temperature trend shows a high, significant correlation over Egypt (Fig. 7b). In addition, a strong negative correlation is observed between winter RH and AMJJ DAOD over Saudi Arabia (Fig. 7c). These findings suggest that trends in DAOD over the EMME region are more strongly related to changes in winter than summer surface temperature and RH. In the next section, we explore the possible reasons for this relationship.

4.4. Soil moisture

Surface air temperature and RH highly impact soil moisture via evaporation, and in turn, soil moisture impacts dust emissions. The spatial distributions of soil moisture trend values from ERA5 and MERRA-2 observations in 2000–2010 and 2010–2017 are shown in Fig. 8. On a regional scale, negative and positive AMJJ soil moisture trends are found in both datasets over the Egypt and Iraq-Syria deserts in the early and late periods, respectively. These trends are thus consistent with those of the DAOD. In addition, the DAOD trends are also consistent with those of winter soil moisture in both the ERA5 and MERRA-2 datasets. The correlation analysis showed that both ERA5 (Fig. 7e, f) and MERRA-2 (Fig. S7) datasets of soil moisture (both AMJJ and winter) and DAOD trends are significantly anti-correlated over deserts in Egypt, in the An-Nafud Desert and in the Iraqi-Syrian deserts (DS1 and DS2, in Fig. 1). Therefore, the analysis reveals that changes in soil moisture is an important influencing factor for dust emissions and DAOD variations over the EMME region even for decadal time scales.

Furthermore, no significant correlations were found between RH, surface temperature, precipitation and soil moisture in summer, thus implying that AMJJ soil moisture levels are mostly affected by the winter meteorological conditions such as SLP, surface temperature and humidity (Fig. S8). Overall, the analysis suggested that meteorological factors in both DJFM and AMJJ have important roles in determining the

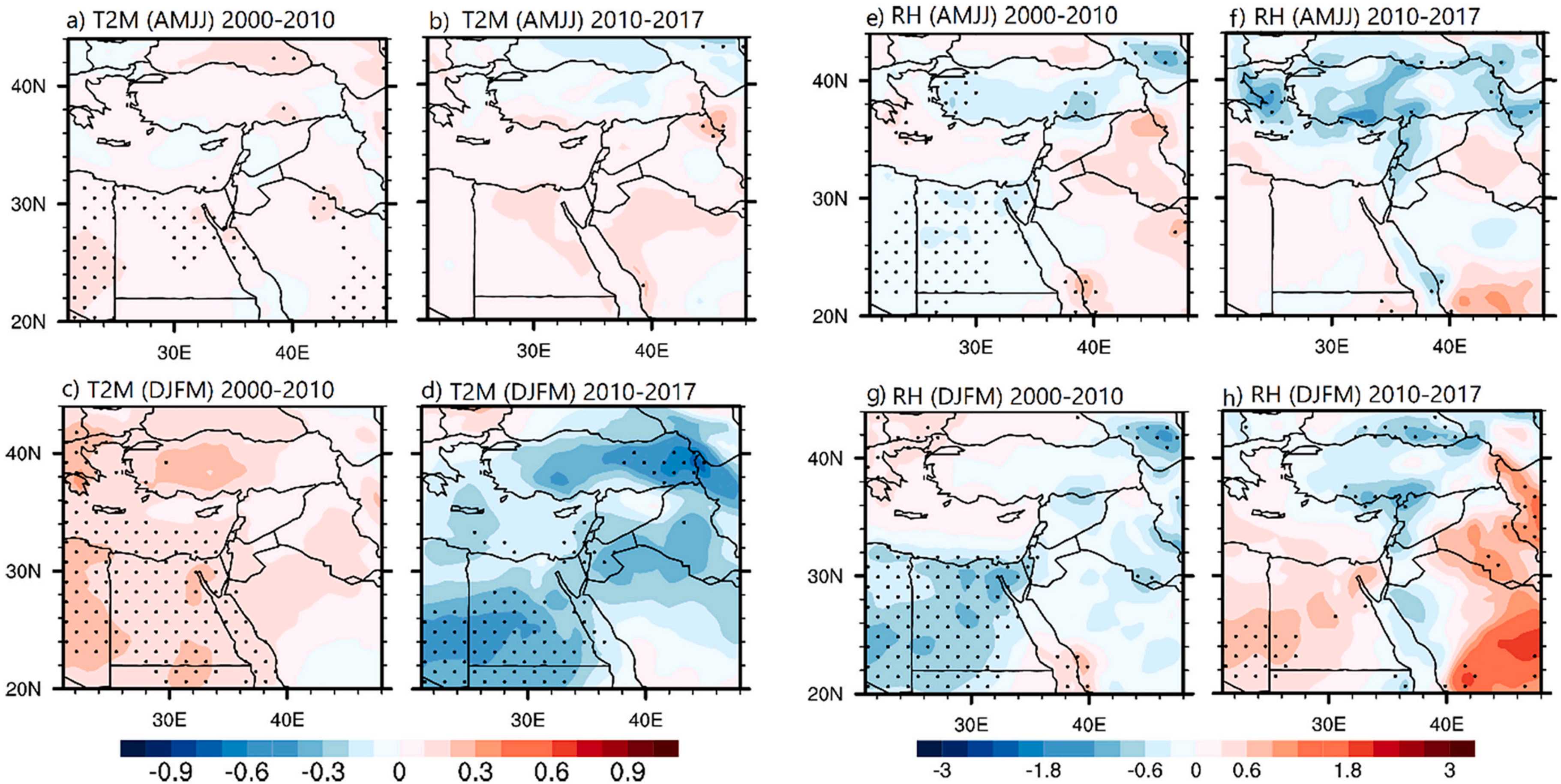

Fig. 6. Spatial distributions of ERA5 surface air temperature linear trends for AMJJ ($^{o}C\ y^{-1}$) during 2000–2010 (a) and 2010–2017 (b), and for DJFM during 2000–2010 (c) and 2010–2017 (d). Spatial distribution of trends in surface RH ($\%\ y^{-1}$) in AMJJ during 2000–2010 (e) and 2010–2017 (f), and for DJFM during 2000–2010 (g) and 2010–2017 (h). Black dots are an indication of the significance of the trends ($p < 0.05$).

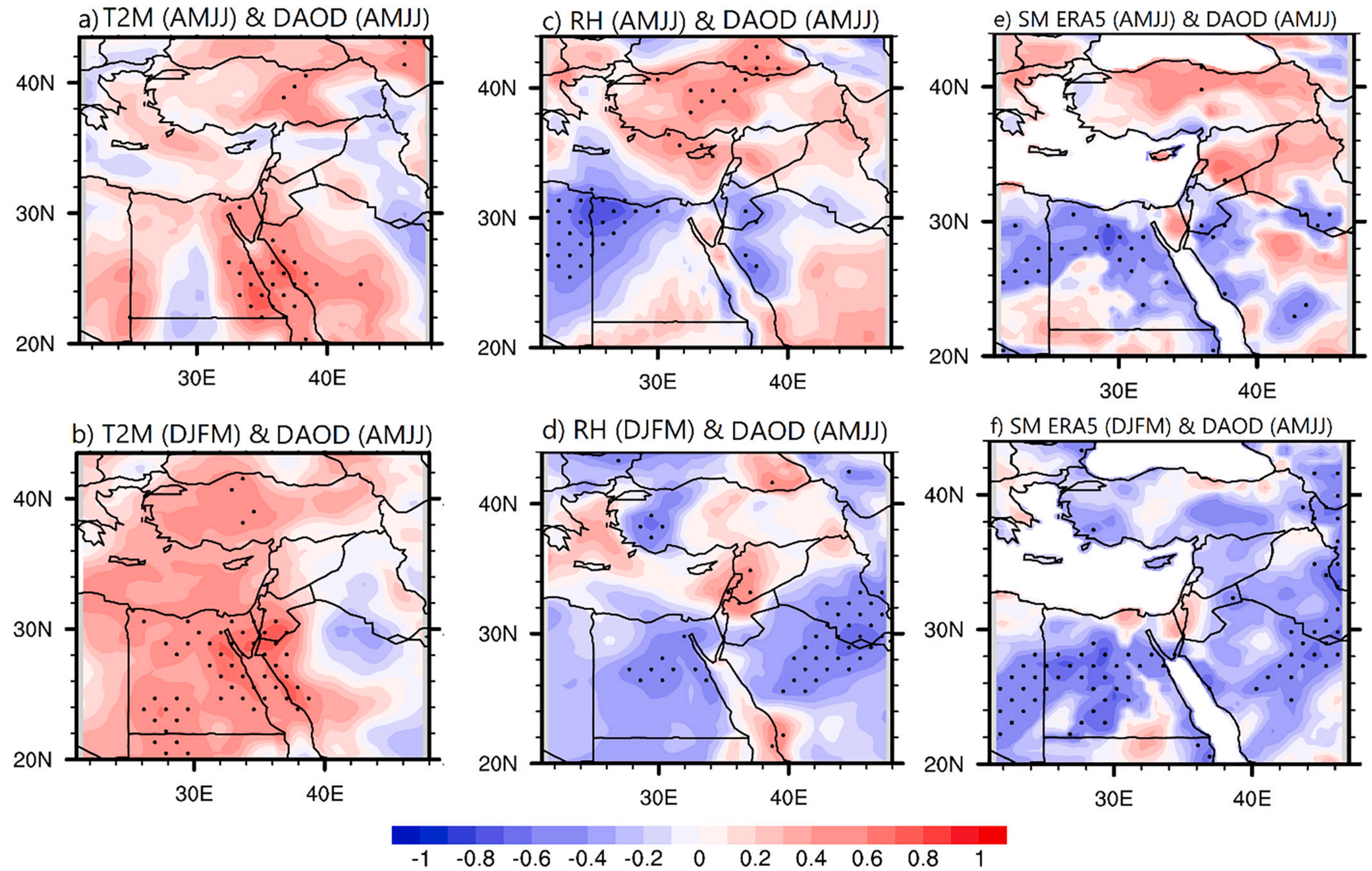

Fig. 7. Distribution of spatial correlations between DAOD and air temperature for the dusty season (AMJJ) (a), between DJFM surface air temperature and subsequent AMJJ DAOD (b), between AMJJ RH and AMJJ DAOD (c), between DJFM surface RH and subsequent AMJJ DAOD (d), between AMJJ DAOD and AMJJ soil moisture (e), and between DJFM soil moisture and subsequent AMJJ DAOD (f). Black dots show statistical significant correlations at 90% confidence level ($p < 0.1$).

AMJJ DAOD trends over EMME, although the analysis did not necessarily recognize the leading and predominant factor, which is the focus of the next section.

5. Multiple linear regression analysis

Using the 6 examined meteorological parameters (soil moisture, SLP, air temperature, wind speed, RH and precipitation) of DJFM and AMJJ, as well as NAOI, as predictors, we constructed Multiple Linear Regression (MLR) models for examining the AMJJ DAOD trends. For each region of interest (DS1 and DS2; Fig. 1), the MLR model can be represented as:

$$y = \beta_0 + \sum_{i=1}^{n} \beta_i x_i + \epsilon \quad (1)$$

here, y represents the mean AMJJ DAOD, x_i is the predictor value for 18 years (2000–2017) i.e., the total years in the calculation period, $\beta_i$is DAOD trend. To evaluate the model's performance, the correlation coefficient R was used determining the significance level at 90%. Note that there may be co-linearities between different predictor variables calculated by this model (Che et al., 2019), and therefore, in order to remove such co-linearities, a Variance Inflation Factor (VIF) is computed by:

$$\mathrm{VIF} = \frac{1}{1 - \mathrm{R_i}^2} \quad (2)$$

where, R_i^2 is the coefficient of determination of the linear regression. As proposed in earlier works, here the VIF was set at threshold value of 10 (Che et al., 2019; Hair et al., 2006).

To investigate the role of each meteorological parameter in DAOD, Pearson's R values between DAOD and meteorological parameters over the DS1 and DS2 for the three periods (i.e., 2000–2017, 2000–2010 and 2010–2017) were calculated. Fig. 9 shows that the AMJJ DAOD was highly affected by wind speed in AMJJ during the three periods over both DS1 and DS2, revealing that dust activity in the EMME region is highly associated with strong wind speeds. The DAOD variability and trends over the examined domains are largely controlled by winter meteorology, including NAOI, SLP, air temperature, RH and soil water content (Fig. 9). Current results are highly consistent with those by Che et al. (2019), who demonstrated that SLP, wind speed, RH and air temperature were successfully used to reproduce the AOD over the dusty regions of the Middle East during 1980–2017.

Time series of the MERRA-2 AMJJ mean DAOD and the MLR model-predicted AMJJ DAOD during 2000–2017 over the two regions of interest (ROI) (dust source 1; DS1, and dust source 2; DS2) are shown in Fig. 10. During 2000–2017, the MLR model can reproduce well the time series of DAOD over the two ROI domains, with R^2 of 0.74 and 0.69 for the DS1 and DS2, respectively and $p < 0.05$ between the predicted and MERRA-2 DAODs.

Finally, the reversal of DAOD trend during 2010–2017 was likely attributed to high SLP in winter combined with NAOI, along with northwesterly winds, which caused an enhancement in RH and soil moisture and a reduction in air temperature over the Middle Eastern desert areas, preventing dust emissions. Similar to our results, DAOD reversal trends observed during 2010–2016 over China, were linked with remarkable changes in wind velocity and soil moisture (Guo et al., 2019). The EMME region has been recognized as one of the most sensitive areas in climate change, with projections of temperature increase, soil moisture and precipitation decrease during the next decades (Zittis et al., 2016, 2022). Under such a climate change scenario, dust activity is

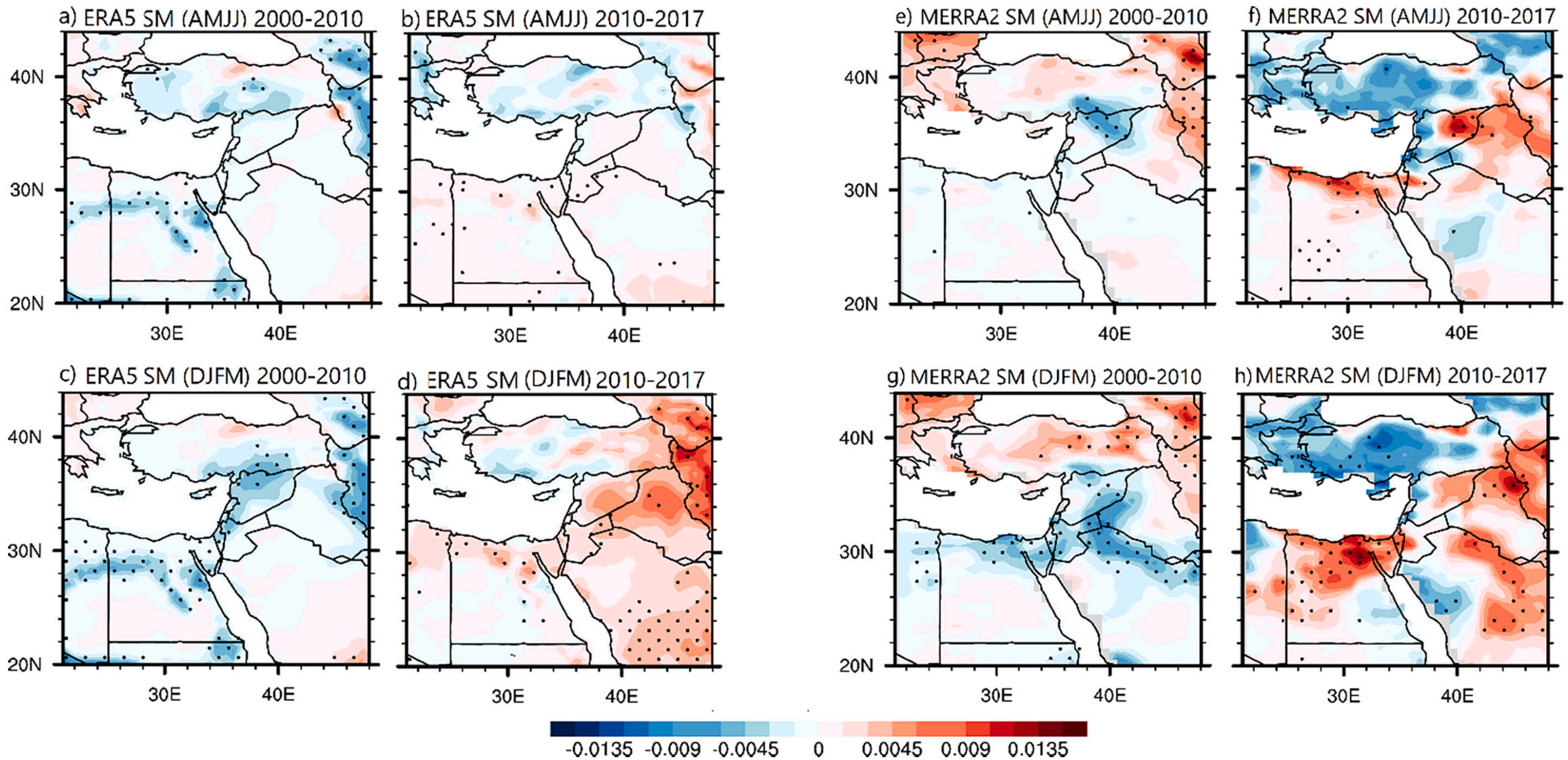

Fig. 8. Spatial distributions of ERA5 soil moisture linear trends (m· m^{-3} yr^{-1}) in AMJJ during 2000–2010 (a) and 2010–2017 (b), and for DJFM during 2000–2010 (c) and 2010–2017 (d). Same analysis for soil moisture trends from MERRA-2 retrievals (e-h). Black dots indicate the statistically significant trends ($p < 0.05$).

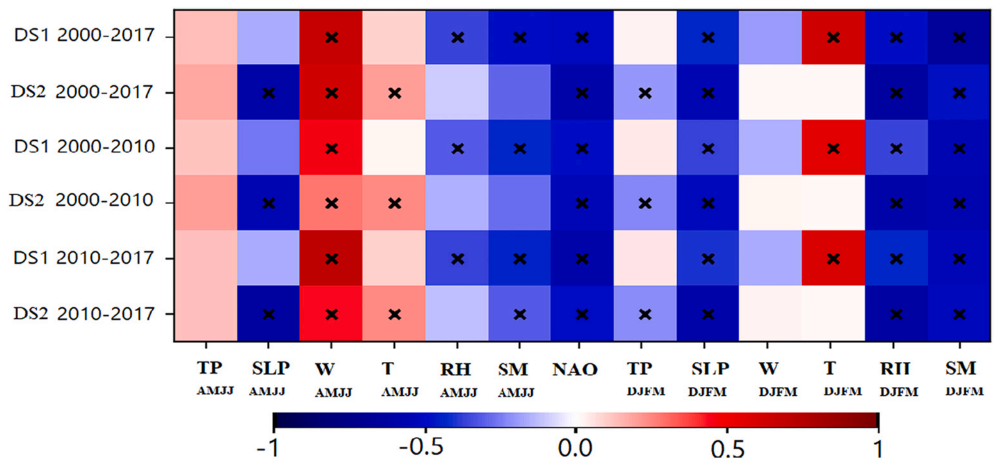

Fig. 9. Pearson correlation coefficient R for spatially averaged MERRA-2 DAOD versus meteorological variables. Colored squares marked with ‘x’ signs indicate R above 90% significance level.

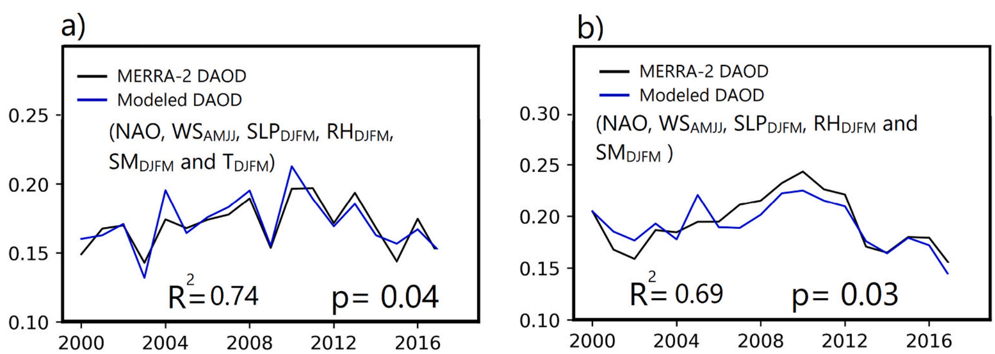

Fig. 10. Time series (2000–2017) of modeled AMJJ DAOD (blue) using the MLR model and mean MERRA-2 DAOD (black) over DS1 (a), and the DS2 (b). (For interpretation of the references to colour in this figure legend, the reader is referred to the web version of this article.)

expected to escalate in the future, necessitating mitigation strategies from the EMME countries against the impacts of dust on socio-economic life, human health and ecosystems.

6. Conclusions

Using aerosol data products from MERRA-2, MODIS and CAMSRA, a significant positive AOD trend was observed in dusty season over the EMME region from 2000 to 2010, followed by a negative aerosol trend between 2010 and 2017. Similar significant AOD trends were also detected in the region at five AERONET sites, revealing an increase and then a decrease in dust activity, which were supported by FMF_{500} and AE variations. This shows that dust acts as the primary dominant factor to the AMJJ AOD trends in the area. In fact, a similar trend was noted between AOD and DAOD values from MERRA-2. The reversal of the DAOD trend was also confirmed using CAMSRA AODs and MERRA-2 dust concentration data.

To investigate the dominant meteorological factors driving the DAOD trends over EMME, we carried out trend along with regression analyses of winter (DJFM) and summer (AMJJ) relevant meteorological variables that affected dust emissions, taken from ERA5 reanalysis, including precipitation, SLP, wind direction and velocity, surface air temperature, soil moisture and RH. DAOD trends over EMME were not so consistent with trends in AMJJ precipitation. Nevertheless, significant negative (during 2001–2010) and positive (during 2010–2017) AMJJ SLP trends were found over the Iraqi and Saudi Arabian deserts, associated with intense southeasterly (2001−2010) and northwesterly (2010–2017) winds. In addition, the trends in winter SLP, surface air temperature and RH were consistent and significantly correlated with the summer DAOD trends. During 2001–2010, a decrease in winter and AMJJ SLP facilitated anomalously hot and dry southeasterly winds towards the arid regions of EMME, which lowered RH and raised air temperature in both the winter and dusty seasons, therefore leading to an increase in evaporation and soil dryness. This was a period of notable increase in dust activity and DAOD over the EMME region.

Conversely, during 2010–2017, anomalously high winter SLP, in conjunction with strong northwesterly winds, caused an enhancement in RH and a reduction in air temperature and evaporation, which raised soil water content in the arid EMME region. Winter soil moisture remained abundant until the following AMJJ season, thereby reducing dust activity. Therefore, over large areas of the EMME region, soil water content could act as a primary factor in determining the dust levels.

Finally, multiple linear regression analysis clearly revealed that over the main dust-source regions, the DAOD variability and trends can be reasonably predicted by winter meteorological variables. The results also highlighted the complex interactions between meteorological drivers and dust generation in the EMME region, and call for further analysis extended to other areas that are highly affected by dust emissions.

CRediT authorship contribution statement

Abdallah Shaheen: Formal analysis, Writing – original draft. **Renguang Wu:** Supervision, Writing – original draft. **Robabeh Yousefi:** Formal analysis, Writing – original draft. **Fang Wang:** Supervision, Writing – original draft. **Quansheng Ge:** Supervision, Writing – original draft. **Dimitris G. Kaskaoutis:** Writing – original draft. **Jun Wang:** Writing – original draft. **Pinhas Alpert:** Writing – original draft. **Iqra Munawar:** Writing – original draft.

Declaration of Competing Interest

The authors declare that they have no known competing financial interests or personal relationships that could have appeared to influence the work reported in this paper.

Data availability

The data that has been used is confidential.

Acknowledgements

Comments of two anonymous reviewers are appreciated. We are grateful to the Earth Observing System Data and Information System (EOSDIS, NASA https://ladsweb.nascom.nasa.gov/), AERONET (https://aeronet.gsfc.nasa.gov), ECMWF (https://ecmwf.int/.), and GMAO (https://disc.gsfc.nasa.gov) for an easy access of data to the scientific community. RW is supported by the National Natural Science Foundation of China grants (41721004, and 41775080). This project is partly supported by National Key Research and Development Program of China (2019YFC0507805), and the Strategic Leading Science and Technology Program of the Chinese Academy of Sciences (XDA20020202).

Appendix A. Supplementary data

Supplementary data to this article can be found online at https://doi.org/10.1016/j.atmosres.2022.106509.

References

Abdelkader, M., Metzger, S., Mamouri, R.E., Astitha, M., Barrie, L., Levin, Z., Lelieveld, J., 2015. Dust–air pollution dynamics over the eastern Mediterranean. Atmos. Chem. Phys. 15, 9173–9189. https://doi.org/10.5194/acp-15-9173-2015.

Achilleos, S., Mouzourides, P., Kalivitis, N., Katra, I., Kloog, I., Kouis, P., Middleton, N., Mihalopoulos, N., Neophytou, M., Panayiotou, A., Papatheodorou, S., Savvides, C., Tymvios, F., Vasiliadou, E., Yiallouros, P., Koutrakis, P., 2020. Spatio-temporal variability of desert dust storms in Eastern Mediterranean (Crete, Cyprus, Israel) between 2006 and 2017 using a uniform methodology. Sci. Total Environ. 714, 136693 https://doi.org/10.1016/j.scitotenv.2020.136693.

Almazroui, M., Alowaibdi, T., Hasanean, H., 2022. Dynamical downscaled CMIP5 scenario–based future climate changes over the Arabian Peninsula. Arab. J. Geosci. 15, 951. https://doi.org/10.1007/s12517-022-10247-7.

Alonso-Perez, S., Cuevas, E., Perez, C., Querol, X., Baldasano, J.M., Draxler, R., De Bustos, J.J., 2011. Trend changes of African airmass intrusions in the marine boundary layer over the subtropical Eastern North Atlantic region in winter. Tellus Ser. B Chem. Phys. Meteorol. 63, 255–265. https://doi.org/10.1111/j.1600-0889.2011.00524.x.

Alpert, P., Barkan, J., Kishcha, P., 2006. A potential climatic index for total Saharan dust: the Sun insolation. J. Geophys. Res. Atmos. 111 https://doi.org/10.1029/2005JD006105.

Alpert, P., Shafir, H., Elhacham, E., 2021. An unknown maximum lag-correlation between rainfall and aerosols at 140–160 minutes. Geophys. Res. Lett. 48 https://doi.org/10.1029/2020GL089334 e2020GL089334.

Barkan, J., Alpert, P., 2008. Synoptic patterns associated with dusty and non-dusty seasons in the Sahara. Theor. Appl. Climatol. 94, 153–162. https://doi.org/10.1007/s00704-007-0354-9.

Barkan, J., Kutiel, H., Alpert, P., 2004. Climatology of dust sources in North Africa and the Arabian Peninsula, based on TOMS data. Indoor Built Environ. 13, 407–419. https://doi.org/10.1177/1420326X04046935.

Baudouin, J.-P., Herzog, M., Petrie, C.A., 2020. Cross-validating precipitation datasets in the Indus River basin. Hydrol. Earth Syst. Sci. 24, 427–450. https://doi.org/10.5194/hess-24-427-2020.

Bryant, R.G., 2013. Recent advances in our understanding of dust source emission processes. Prog. Phys. Geogr. Earth Environ. 37, 397–421. https://doi.org/10.1177/0309133313479391.

Buchard, V., Randles, C.A., da Silva, A.M., Darmenov, A., Colarco, P.R., Govindaraju, R., Ferrare, R., Hair, J., Beyersdorf, A.J., Ziemba, L.D., Yu, H., 2017. The MERRA-2 aerosol reanalysis, 1980 onward. Part II: evaluation and case studies. J. Clim. 30, 6851–6872. https://doi.org/10.1175/jcli-d-16-0613.1.

Che, H., Gui, K., Xia, X., Wang, Y., Holben, B.N., Goloub, P., Cuevas-Agullo, E., Wang, H., Zheng, Y., Zhao, H., Zhang, X., 2019. Large contribution of meteorological factors to inter-decadal changes in regional aerosol optical depth. Atmos. Chem. Phys. 19, 10497–10523. https://doi.org/10.5194/acp-19-10497-2019.

Dayan, U., Ziv, B., Shoob, T., Enzel, Y., 2008. Suspended dust over southeastern Mediterranean and its relation to atmospheric circulations. Int. J. Climatol. 28, 915–924. https://doi.org/10.1002/joc.1587.

DeMott, P.J., Prenni, A.J., Liu, X., Kreidenweis, S.M., Petters, M.D., Twohy, C.H., Richardson, M.S., Eidhammer, T., Rogers, D.C., 2010. Predicting global atmospheric ice nuclei distributions and their impacts on climate. Proc. Natl. Acad. Sci. 107, 11217–11222. https://doi.org/10.1073/pnas.0910818107.

Elhacham, E., Alpert, P., 2016. Impact of coastline-intensive anthropogenic activities on the atmosphere from moderate resolution imaging spectroradiometer (MODIS) data in Dubai (2001–2014). Earth's Futur. 4, 54–61. https://doi.org/10.1002/2015EF000325.

Elhacham, E., Alpert, P., 2020. Potential new aerosol source(s) in the Middle East. Sci. Total Environ. 726, 137925 https://doi.org/10.1016/j.scitotenv.2020.137925.

Engelstaedter, S., Tegen, I., Washington, R., 2006. North African dust emissions and transport. Earth-Sci. Rev. 79, 73–100. https://doi.org/10.1016/j.earscirev.2006.06.004.

Flemming, J., Huijnen, V., Arteta, J., Bechtold, P., Beljaars, A., Blechschmidt, A.-M., Diamantakis, M., Engelen, R.J., Gaudel, A., Inness, A., Jones, L., Josse, B., Katragkou, E., Marecal, V., Peuch, V.-H., Richter, A., Schultz, M.G., Stein, O., Tsikerdekis, A., 2015. Tropospheric chemistry in the integrated forecasting system of ECMWF. Geosci. Model Dev. 8, 975–1003. https://doi.org/10.5194/gmd-8-975-2015.

Floutsi, A.A., Korras-Carraca, M.B., Matsoukas, C., Hatzianastassiou, N., Biskos, G., 2016. Climatology and trends of aerosol optical depth over the Mediterranean basin during the last 12years (2002–2014) based on Collection 006 MODIS-Aqua data. Sci. Total Environ. 551–552, 292–303. https://doi.org/10.1016/j.scitotenv.2016.01.192.

Foltz, G.R., McPhaden, M.J., 2008. Impact of Saharan Dust on Tropical North Atlantic SST*. J. Clim. 21, 5048–5060. https://doi.org/10.1175/2008JCLI2232.1.

Francis, D., Alshamsi, N., Cuesta, J., Gokcen Isik, A., Dundar, C., 2019. Cyclogenesis and density currents in the Middle East and the associated dust activity in September 2015. Geosci. https://doi.org/10.3390/geosciences9090376.

Francis, D., Fonseca, R., Nelli, N., Cuesta, J., Weston, M., Evan, A., Temimi, M., 2020. The atmospheric drivers of the major Saharan dust storm in June 2020. Geophys. Res. Lett. 47 https://doi.org/10.1029/2020GL090102 e2020GL090102.

Francis, D., Chaboureau, J.-P., Nelli, N., Cuesta, J., Alshamsi, N., Temimi, M., Pauluis, O., Xue, L., 2021. Summertime dust storms over the Arabian Peninsula and impacts on radiation, circulation, cloud development and rain. Atmos. Res. 250, 105364 https://doi.org/10.1016/j.atmosres.2020.105364.

Furman, H.K.H., 2003. Dust storms in the Middle East: sources of origin and their temporal characteristics. Indoor Built Environ. 12, 419–426. https://doi.org/10.1177/1420326X03037110.

Gandham, H., Dasari, H.P., Langodan, S., Karumuri, R.K., Hoteit, I., 2020. Major changes in extreme dust events dynamics over the Arabian Peninsula during 2003–2017 driven by atmospheric conditions. J. Geophys. Res. https://doi.org/10.1029/2020JD032931.

Ganor, E., Osetinsky, I., Stupp, A., Alpert, P., 2010. Increasing trend of African dust, over 49 years, in the eastern Mediterranean. J. Geophys. Res. Atmos. 115 https://doi.org/10.1029/2009JD012500.

Gelaro, R., McCarty, W., Suárez, M.J., Todling, R., Molod, A., Takacs, L., Randles, C.A., Darmenov, A., Bosilovich, M.G., Reichle, R., Wargan, K., Coy, L., Cullather, R., Draper, C., Akella, S., Buchard, V., Conaty, A., da Silva, A.M., Gu, W., Kim, G.-K., Koster, R., Lucchesi, R., Merkova, D., Nielsen, J.E., Partyka, G., Pawson, S., Putman, W., Rienecker, M., Schubert, S.D., Sienkiewicz, M., Zhao, B., 2017. The modern-era retrospective analysis for research and applications, version 2 (MERRA-2). J. Clim. 30, 5419–5454. https://doi.org/10.1175/jcli-d-16-0758.1.

Georgoulias, A.K., Alexandri, G., Kourtidis, K.A., Lelieveld, J., Zanis, P., Pöschl, U., Levy, R., Amiridis, V., Marinou, E., Tsikerdekis, A., 2016. Spatiotemporal variability and contribution of different aerosol types to the aerosol optical depth over the Eastern Mediterranean. Atmos. Chem. Phys. 16, 13853–13884. https://doi.org/10.5194/acp-16-13853-2016.

Gholami, H., Mohamadifar, A., Rahimi, S., Kaskaoutis, D.G., Collins, A.L., 2021. Predicting land susceptibility to atmospheric dust emissions in Central Iran by combining integrated data mining and a regional climate model. Atmos. Poll. Res. 12, 172–187. https://doi.org/10.1016/j.apr.2021.03.005.

Ginoux, P., Prospero, J.M., Torres, O., Chin, M., 2004. Long-term simulation of global dust distribution with the GOCART model: correlation with North Atlantic Oscillation. Environ. Model. Softw. 19, 113–128. https://doi.org/10.1016/S1364-8152(03)00114-2.

Gleixner, S., Demissie, T., Diro, G.T., 2020. Did ERA5 improve temperature and precipitation reanalysis over East Africa? Atmos. https://doi.org/10.3390/atmos11090996.

Gui, K., Che, H., Wang, Y., Wang, H., Zhang, L., Zhao, H., Zheng, Y., Sun, T., Zhang, X., 2019. Satellite-derived PM2.5 concentration trends over Eastern China from 1998 to 2016: relationships to emissions and meteorological parameters. Environ. Pollut. 247, 1125–1133. https://doi.org/10.1016/j.envpol.2019.01.056.

Gui, K., Che, H., Zheng, Y., Zhao, H., Yao, W., Li, L., Zhang, L., Wang, H., Wang, Y., Zhang, X., 2021a. Three-dimensional climatology, trends, and meteorological drivers of global and regional tropospheric type-dependent aerosols: insights from 13 years (2007–2019) of CALIOP observations. Atmos. Chem. Phys. 21, 15309–15336. https://doi.org/10.5194/acp-21-15309-2021.

Gui, K., Che, H., Wang, Y., Xia, X., Holben, B.N., Goloub, P., Cuevas-Agulló, E., Yao, W., Zheng, Y., Zhao, H., Li, L., Zhang, X., 2021b. A global-scale analysis of the MISR

Level-3 aerosol optical depth (AOD) product: comparison with multi-platform AOD data sources. Atmos. Pollut. Res. 12, 101238 https://doi.org/10.1016/j.apr.2021.101238.
Gui, K., Che, H., Li, L., Zheng, Y., Zhang, L., Zhao, H., Zhong, J., Yao, W., Liang, Y., Wang, Y., Zhang, X., 2022. The significant contribution of small-sized and spherical aerosol particles to the decreasing trend in total aerosol optical depth over land from 2003 to 2018. Engineering. https://doi.org/10.1016/j.eng.2021.05.017.
Guo, J., Xu, H., Liu, L., Chen, D., Peng, Y., Yim, S.H.-L., Yang, Y., Li, J., Zhao, C., Zhai, P., 2019. The trend reversal of dust aerosol over East Asia and the North Pacific ocean attributed to large-scale meteorology, deposition, and soil moisture. J. Geophys. Res. Atmos. 124, 10450–10466. https://doi.org/10.1029/2019JD030654.
Hair, J.F., Black, W.C., Babin, B.J., Anderson, R.E., Tatham, R., 2006. Multivariate Data Analysis. Pearson Education, New Jersey Hoboken.
Hamidi, M., Kavianpour, M.R., Shao, Y., 2013. Synoptic analysis of dust storms in the Middle East. Asia-Pacific J. Atmos. Sci. 49, 279–286. https://doi.org/10.1007/s13143-013-0027-9.
Hamidianpour, M., Jahanshahi, S.M.A., Kaskaoutis, D.G., Rashki, A., Nastos, P.G., 2021. Climatology of the Sistan Levar wind: atmospheric dynamics driving its onset, duration and withdrawal. Atmos. Res. 260, 105711 https://doi.org/10.1016/j.atmosres.2021.105711.
Hamzeh, N.H., Kaskaoutis, D.G., Rashki, A., Mohammadpour, K., 2021. Long-term variability of dust events in Southwestern Iran and its relationship with the drought. Atmos. https://doi.org/10.3390/atmos12101350.
Hersbach, H., Bell, B., Berrisford, P., Hirahara, S., Horányi, A., Muñoz-Sabater, J., Nicolas, J., Peubey, C., Radu, R., Schepers, D., Simmons, A., Soci, C., Abdalla, S., Abellan, X., Balsamo, G., Bechtold, P., Biavati, G., Bidlot, J., Bonavita, M., De Chiara, G., Dahlgren, P., Dee, D., Diamantakis, M., Dragani, R., Flemming, J., Forbes, R., Fuentes, M., Geer, A., Haimberger, L., Healy, S., Hogan, R.J., Hólm, E., Janisková, M., Keeley, S., Laloyaux, P., Lopez, P., Lupu, C., Radnoti, G., de Rosnay, P., Rozum, I., Vamborg, F., Villaume, S., Thépaut, J.-N., 2020. The ERA5 global reanalysis. Q. J. R. Meteorol. Soc. 146, 1999–2049. https://doi.org/10.1002/qj.3803.
Holben, B.N., Eck, T.F., Slutsker, I., Tanre, D., Buis, J.P., Setzer, A., Vermote, E., Reagan, J.A., Kaufman, Y.J., Nakajima, T., Lavenu, F., Jankowiak, I., Smirnov, A., 1998. AERONET - a federated instrument network and data archive for aerosol characterization. Remote Sens. Environ. 66, 1–16. https://doi.org/10.1016/s0034-4257(98)00031-5.
Hsu, N.C., Gautam, R., Sayer, A.M., Bettenhausen, C., Li, C., Jeong, M.J., Tsay, S.C., Holben, B.N., 2012. Global and regional trends of aerosol optical depth over land and ocean using SeaWiFS measurements from 1997 to 2010. Atmos. Chem. Phys. 12, 8037–8053. https://doi.org/10.5194/acp-12-8037-2012.
Huneeus, N., Schulz, M., Balkanski, Y., Griesfeller, J., Prospero, J., Kinne, S., Bauer, S., Boucher, O., Chin, M., Dentener, F., Diehl, T., Easter, R., Fillmore, D., Ghan, S., Ginoux, P., Grini, A., Horowitz, L., Koch, D., Krol, M.C., Landing, W., Liu, X., Mahowald, N., Miller, R., Morcrette, J.-J., Myhre, G., Penner, J., Perlwitz, J., Stier, P., Takemura, T., Zender, C.S., 2011. Global dust model intercomparison in AeroCom phase I. Atmos. Chem. Phys. 11, 7781–7816. https://doi.org/10.5194/acp-11-7781-2011.
Hurrel, J.W., 1995. Decadal trends in the North Atlantic Oscillation and relations to regional temperature and precipitation. Science 269, 676–679.
Inness, A., Ades, M., Agusti-Panareda, A., Barré, J., Benedictow, A., Blechschmidt, A.-M., Dominguez, J.J., Engelen, R., Eskes, H., Flemming, J., Huijnen, V., Jones, L., Kipling, Z., Massart, S., Parrington, M., Peuch, V.-H., Razinger, M., Remy, S., Schulz, M., Suttie, M., 2019. The CAMS reanalysis of atmospheric composition. Atmos. Chem. Phys. 19, 3515–3556. https://doi.org/10.5194/acp-19-3515-2019.
Jiang, J.H., Su, H., Huang, L., Wang, Y., Massie, S., Zhao, B., Omar, A., Wang, Z., 2018. Contrasting effects on deep convective clouds by different types of aerosols. Nat. Commun. 9, 3874. https://doi.org/10.1038/s41467-018-06280-4.
Jickells, T.D., An, Z.S., Andersen, K.K., Baker, A.R., Bergametti, G., Brooks, N., Cao, J.J., Boyd, P.W., Duce, R.A., Hunter, K.A., Kawahata, H., Kubilay, N., laRoche, J., Liss, P. S., Mahowald, N., Prospero, J.M., Ridgwell, A.J., Tegen, I., Torres, R., 2005. Global iron connections between desert dust, ocean biogeochemistry, and climate. Science 308, 67–71. https://doi.org/10.1126/science.1105959.
Jin, Q., Wei, J., Yang, Z.-L., Pu, B., Huang, J., 2015. Consistent response of Indian summer monsoon to Middle East dust in observations and simulations. Atmos. Chem. Phys. 15, 9897–9915.
Kalita, G., Kunchala, R.K., Fadnavis, S., Kaskaoutis, D.G., 2020. Long term variability of carbonaceous aerosols over Southeast Asia via reanalysis: association with changes in vegetation cover and biomass burning. Atmos. Res. 245, 105064 https://doi.org/10.1016/j.atmosres.2020.105064.
Kaskaoutis, D.G., Houssos, E.E., Rashki, A., Francois, P., Legrand, M., Goto, D., Bartzokas, A., Kambezidis, H.D., Takemura, T., 2016. The Caspian Sea–Hindu Kush Index (CasHKI): a regulatory factor for dust activity over southwest Asia. Glob. Planet. Chang. 137, 10–23. https://doi.org/10.1016/j.gloplacha.2015.12.011.
Kaskaoutis, D.G., Rashki, A., Dumka, U.C., Mofidi, A., Kambezidis, H.D., Psiloglou, B.E., Karagiannis, D., Petrinoli, K., Gavriil, A., 2019. Atmospheric dynamics associated with exceptionally dusty conditions over the eastern Mediterranean and Greece in March 2018. Atmos. Res. 218, 269–284. https://doi.org/10.1016/j.atmosres.2018.12.009.
King, M.D., Menzel, W.P., Kaufman, Y.J., Tanre, D., Gao, Bo-Cai, Platnick, S., Ackerman, S.A., Remer, L.A., Pincus, R., Hubanks, P.A., 2003. Cloud and aerosol properties, precipitable water, and profiles of temperature and water vapor from MODIS. IEEE Trans. Geosci. Remote Sens. 41, 442–458. https://doi.org/10.1109/TGRS.2002.808226.
Klingmüller, K., Pozzer, A., Metzger, S., Stenchikov, G.L., Lelieveld, J., 2016. Aerosol optical depth trend over the Middle East. Atmos. Chem. Phys. 16, 5063–5073. https://doi.org/10.5194/acp-16-5063-2016.
Krasnov, H., Katra, I., Friger, M., 2016. Increase in dust storm related PM10 concentrations: a time series analysis of 2001–2015. Environ. Pollut. 213, 36–42. https://doi.org/10.1016/j.envpol.2015.10.021.
Krichak, S.O., Alpert, P., 2022. The role of the Near East surface pressure variations in recent past trends of wet season precipitation in the Levant. Int. J. Climatol. https://doi.org/10.1002/joc.7632 n/a.
Labban, A.H., Mashat, A.-W.S., Awad, A.M., 2021. The variability of the Siberian high ridge over the Middle East. Int. J. Climatol. 41, 104–130. https://doi.org/10.1002/joc.6611.
Lee, S., Pinhas, A., Alexandra, C.A., 2020. Aerosol pattern changes over the dead sea from west to east - using high-resolution satellite data. Atmos. Environ. 243, 117737 https://doi.org/10.1016/j.atmosenv.2020.117737.
Liu, H., Yan, R., Yang, J., 2021. Credibility and statistical characteristics of CAMSRA and MERRA-2 AOD reanalysis products over the Sichuan Basin during 2003–2018. Atmos. Environ. 244, 117980 https://doi.org/10.1016/j.atmosenv.2020.117980.
Marinou, E., Amiridis, V., Binietoglou, I., Tsikerdekis, A., Solomos, S., Proestakis, E., Konsta, D., Papagiannopoulos, N., Tsekeri, A., Vlastou, G., Zanis, P., Balis, D., Wandinger, U., Ansmann, A., 2017. Three-dimensional evolution of Saharan dust transport towards Europe based on a 9-year EARLINET-optimized CALIPSO dataset. Atmos. Chem. Phys. 17, 5893–5919. https://doi.org/10.5194/acp-17-5893-2017.
Mohammadpour, K., Sciortino, M., Kaskaoutis, D.G., 2021. Classification of weather clusters over the Middle East associated with high atmospheric dust-AODs in West Iran. Atmos. Res. 259, 105682 https://doi.org/10.1016/j.atmosres.2021.105682.
Nabat, P., Somot, S., Mallet, M., Sanchez-Lorenzo, A., Wild, M., 2014. Contribution of anthropogenic sulfate aerosols to the changing Euro-Mediterranean climate since 1980. Geophys. Res. Lett. 41, 5605–5611. https://doi.org/10.1002/2014GL060798.
Nabat, P., Somot, S., Cassou, C., Mallet, M., Michou, M., Bouniol, D., Decharme, B., Drugé, T., Roehrig, R., Saint-Martin, D., 2020. Modulation of radiative aerosols effects by atmospheric circulation over the Euro-Mediterranean region. Atmos. Chem. Phys. 20, 8315–8349. https://doi.org/10.5194/acp-20-8315-2020.
Notaro, M., Yu, Y., Kalashnikova, O.V., 2015. Regime shift in Arabian dust activity, triggered by persistent Fertile Crescent drought. J. Geophys. Res. Atmos. 120, 10,210–229,249. https://doi.org/10.1002/2015JD023855.
Papadimas, C.D., Hatzianastassiou, N., Mihalopoulos, N., Querol, X., Vardavas, I., 2008. Spatial and temporal variability in aerosol properties over the Mediterranean basin based on 6-year (2000–2006) MODIS data. J. Geophys. Res. Atmos. 113 https://doi.org/10.1029/2007JD009189.
Papadimas, C.D., Hatzianastassiou, N., Matsoukas, C., Kanakidou, M., Mihalopoulos, N., Vardavas, I., 2012. The direct effect of aerosols on solar radiation over the broader Mediterranean basin. Atmos. Chem. Phys. 12, 7165–7185. https://doi.org/10.5194/acp-12-7165-2012.
Parajuli, S.P., Stenchikov, G.L., Ukhov, A., Kim, H., 2019. Dust emission modeling using a new high-resolution dust source function in WRF-chem with implications for air quality. J. Geophys. Res. Atmos. 124, 10109–10133. https://doi.org/10.1029/2019JD030248.
Pey, J., Querol, X., Alastuey, A., Forastiere, F., Stafoggia, M., 2013. African dust outbreaks over the Mediterranean Basin during 2001–2011: PM$_{10}$ concentrations, phenomenology and trends, and its relation with synoptic and mesoscale meteorology. Atmos. Chem. Phys. 13, 1395–1410. https://doi.org/10.5194/acp-13-1395-2013.
Pozzer, A., de Meij, A., Yoon, J., Tost, H., Georgoulias, A.K., Astitha, M., 2015. AOD trends during 2001–2010 from observations and model simulations. Atmos. Chem. Phys. 15, 5521–5535. https://doi.org/10.5194/acp-15-5521-2015.
Provençal, S., Kishcha, P., da Silva, A.M., Elhacham, E., Alpert, P., 2017. AOD distributions and trends of major aerosol species over a selection of the world's most populated cities based on the 1st version of NASA's MERRA Aerosol Reanalysis. Urban Clim. 20, 168–191. https://doi.org/10.1016/j.uclim.2017.04.001.
Rashki, A., Kaskaoutis, D.G., de Rautenbach, C.J.W., Eriksson, P.G., Qiang, M., Gupta, P., 2012. Dust storms and their horizontal dust loading in the Sistan region, Iran. Aeolian Res. 5, 51–62. https://doi.org/10.1016/j.aeolia.2011.12.001.
Remer, L.A., Kaufman, Y.J., Tanré, D., Mattoo, S., Chu, D.A., Martins, J.V., Li, R.R., Ichoku, C., Levy, R.C., Kleidman, R.G., Eck, T.F., Vermote, E., Holben, B.N., 2005. The MODIS aerosol algorithm, products, and validation. J. Atmos. Sci. 62, 947–973. https://doi.org/10.1175/JAS3385.1.
Rosenfeld, D., 2019. Aerosol-driven droplet concentrations dominate coverage and water of oceanic low-level clouds (vol 364, eaay4194, 2019). Science 365, 230.
Salvador, P., Alonso-Pérez, S., Pey, J., Artiñano, B., de Bustos, J.J., Alastuey, A., Querol, X., 2014. African dust outbreaks over the western Mediterranean Basin: 11-year characterization of atmospheric circulation patterns and dust source areas. Atmos. Chem. Phys. 14, 6759–6775. https://doi.org/10.5194/acp-14-6759-2014.
Schepanski, K., Tegen, I., Macke, A., 2009. Saharan dust transport and deposition towards the tropical northern Atlantic. Atmos. Chem. Phys. 9, 1173–1189. https://doi.org/10.5194/acp-9-1173-2009.
Schepanski, K., Mallet, M., Heinold, B., Ulrich, M., 2016. North African dust transport toward the western Mediterranean basin: atmospheric controls on dust source activation and\hack{\newline} transport pathways during June–July~2013. Atmos. Chem. Phys. 16, 14147–14168. https://doi.org/10.5194/acp-16-14147-2016.
Sciare, J., Bardouki, H., Moulin, C., Mihalopoulos, N., 2003. Aerosol sources and their contribution to the chemical composition of aerosols in the Eastern Mediterranean Sea during summertime. Atmos. Chem. Phys. 3, 291–302. https://doi.org/10.5194/acp-3-291-2003.
Shaheen, A., 2020. A new MODIS C6.1 and MERRA-2 merged aerosol products: Validation over the Eastern Mediterranean Region. In: EGU General Assembly

Conference Abstracts. AA(Center for Monsoon System Research). Institute of Atmospheric Physics, University of Chinese Academy of Sciences, Beijing, China, p. 639. https://doi.org/10.5194/egusphere-egu2020-639.

Shaheen, A., Kidwai, A.A., Ain, N.U., Aldabash, M., Zeeshan, A., 2017. Estimating air particulate matter 10 using landsat multi-temporal data and analyzing its annual temporal pattern over gaza strip. Palestine. J. Asian Sci. Res. 7, 22–37. https://doi.org/10.18488/journal.2/2017.7.2/2.2.22.37.

Shaheen, A., Wu, R., Aldabash, M., 2020. Long-term AOD trend assessment over the Eastern Mediterranean region: a comparative study including a new merged aerosol product. Atmos. Environ. 238, 117736 https://doi.org/10.1016/j.atmosenv.2020.117736.

Shaheen, A., Wu, R., Lelieveld, J., Yousefi, R., Aldabash, M., 2021a. Winter AOD trend changes over the Eastern Mediterranean and Middle East region. Int. J. Climatol. 41, 5516–5535. https://doi.org/10.1002/joc.7139.

Shaheen, A., Wu, R., Yousefi, R., 2021b. Dust aerosol trends over the Eastern Mediterranean region during 2003-2019. In: EGU General Assembly Conference Abstracts, EGU General Assembly Conference Abstracts. https://doi.org/10.5194/egusphere-egu21-582 pp. EGU21-582.

Shao, Y., Raupach, M.R., Findlater, P.A., 1993. Effect of saltation bombardment on the entrainment of dust by wind. J. Geophys. Res. Atmos. 98, 12719–12726. https://doi.org/10.1029/93JD00396.

Shi, H., Xiao, Z., Zhan, X., Ma, H., Tian, X., 2019. Evaluation of MODIS and two reanalysis aerosol optical depth products over AERONET sites. Atmos. Res. 220, 75–80.

Solmon, F., Nair, V.S., Mallet, M., 2015. Increasing Arabian dust activity and the Indian summer monsoon. Atmos. Chem. Phys. 15, 8051–8064.

Solomos, S., Kalivitis, N., Mihalopoulos, N., Amiridis, V., Kouvarakis, G., Gkikas, A., Binietoglou, I., Tsekeri, A., Kazadzis, S., Kottas, M., Pradhan, Y., Proestakis, E., Nastos, P.T., Marenco, F., 2018. From tropospheric folding to Khamsin and Foehn Winds: how atmospheric dynamics advanced a record-breaking dust episode in Crete. Atmos. https://doi.org/10.3390/atmos9070240.

Tarek, M., Brissette, F.P., Arsenault, R., 2020. Evaluation of the ERA5 reanalysis as a potential reference dataset for hydrological modelling over North America. Hydrol. Earth Syst. Sci. 24, 2527–2544. https://doi.org/10.5194/hess-24-2527-2020.

Thiagarajan, N., Aeolus Lee, C.-T., 2004. Trace-element evidence for the origin of desert varnish by direct aqueous atmospheric deposition. Earth Planet. Sci. Lett. 224, 131–141. https://doi.org/10.1016/j.epsl.2004.04.038.

Tutsak, E., Koçak, M., 2020. Optical and microphysical properties of the columnar Aerosol burden over the Eastern Mediterranean: Discrimination of Aerosol types. Atmos. Environ. 229, 117463 https://doi.org/10.1016/j.atmosenv.2020.117463.

Ukhov, A., Mostamandi, S., da Silva, A., Flemming, J., Alshehri, Y., Shevchenko, I., Stenchikov, G., 2020. Assessment of natural and anthropogenic aerosol air pollution in the Middle East using MERRA-2, CAMS data assimilation products, and high-resolution WRF-Chem model simulations. Atmos. Chem. Phys. 20, 9281–9310.

Wang, C., Graham, R.M., Wang, K., Gerland, S., Granskog, M.A., 2019. Comparison of ERA5 and ERA-interim near-surface air temperature, snowfall and precipitation over Arctic Sea ice: effects on sea ice thermodynamics and evolution. Cryosph. 13, 1661–1679. https://doi.org/10.5194/tc-13-1661-2019.

Wu, R., Wen, Z., He, Z., 2013. ENSO contribution to aerosol variations over the maritime continent and the Western North Pacific during 2000–10. J. Clim. 26, 6541–6560. https://doi.org/10.1175/JCLI-D-12-00253.1.

Yoon, J., Burrows, J.P., Vountas, M., von Hoyningen-Huene, W., Chang, D.Y., Richter, A., Hilboll, A., 2014. Changes in atmospheric aerosol loading retrieved from space-based measurements during the past decade. Atmos. Chem. Phys. 14, 6881–6902. https://doi.org/10.5194/acp-14-6881-2014.

Yousefi, R., Wang, F., Ge, Q., Shaheen, A., 2020a. Long-term aerosol optical depth trend over Iran and identification of dominant aerosol types. Sci. Total Environ. 722, 137906 https://doi.org/10.1016/j.scitotenv.2020.137906.

Yousefi, R., Wang, F., Ge, Q., Shaheen, A., Luterbacher, J., 2020b. Long-term AOD trend analysis and classification of major aerosol types over Iran from 1980 to 2018. In: EGU General Assembly Conference Abstracts, p. 1831. https://doi.org/10.5194/egusphere-egu2020-1831.

Yousefi, R., Wang, F., Ge, Q., Lelieveld, J., Shaheen, A., 2021a. Aerosol trends during the dusty season over Iran. Remote Sens. https://doi.org/10.3390/rs13061045.

Yousefi, R., Wang, F., Ge, Q., Shaheen, A., 2021b. Contribution of meteorological factors to AOD variability during the dusty season over Iran. In: EGU General Assembly Conference Abstracts, EGU General Assembly Conference Abstracts. https://doi.org/10.5194/egusphere-egu21-1349 pp. EGU21-1349.

Yu, Y., Notaro, M., Liu, Z., Wang, F., Alkolibi, F., Fadda, E., Bakhrjy, F., 2015. Climatic controls on the interannual to decadal variability in Saudi Arabian dust activity: toward the development of a seasonal dust prediction model. J. Geophys. Res. Atmos. 120, 1739–1758. https://doi.org/10.1002/2014JD022611.

Yu, Y., Notaro, M., Kalashnikova, O.V., Garay, M.J., 2016. Climatology of summer Shamal wind in the Middle East. J. Geophys. Res. Atmos. 121, 289–305. https://doi.org/10.1002/2015JD024063.

Yu, Y., Kalashnikova, O.V., Garay, M.J., Lee, H., Notaro, M., 2018. Identification and characterization of dust source regions across North Africa and the Middle East using MISR satellite observations. Geophys. Res. Lett. 45, 6690–6701. https://doi.org/10.1029/2018GL078324.

Zhao, Y., Huang, A., Zhu, X., Zhou, Y., Huang, Y., 2013. The impact of the winter North Atlantic Oscillation on the frequency of spring dust storms over Tarim Basin in Northwest China in the past half-century. Environ. Res. Lett. 8, 24026. https://doi.org/10.1088/1748-9326/8/2/024026.

Zittis, G., Hadjinicolaou, P., Fnais, M., Lelieveld, J., 2016. Projected changes in heat wave characteristics in the eastern Mediterranean and the Middle East. Reg. Environ. Chang. 16, 1863–1876. https://doi.org/10.1007/s10113-014-0753-2.

Zittis, G., Almazroui, M., Alpert, P., Ciais, P., Cramer, W., Dahdal, Y., Fnais, M., Francis, D., Hadjinicolaou, P., Howari, F., Jrrar, A., Kaskaoutis, D.G., Kulmala, M., Lazoglou, G., Mihalopoulos, N., Lin, X., Rudich, Y., Sciare, J., Stenchikov, G., Xoplaki, E., Lelieveld, J., 2022. Climate change and weather extremes in the Eastern Mediterranean and Middle East. Rev. Geophys. 60 https://doi.org/10.1029/2021RG000762 e2021RG000762.